AirCargoChallenge 2022

Technical Report

Team #27

LeanIng Project

LEANING PROJECT

1 SUMMARY

2 INTRODUCTION

This report has the purpose of describing the main design features of a model aircraft developed to compete in the Air Cargo Challenge 2022, an international aeronautical engineering competition targeted at university students and research associates.

Our team, called *LeanIng Project*, was established in Pisa, Italy, on the 1st of November 2020 and it is composed of 13 members divided into different working groups.

Previously, the University of Pisa participated in 2009, 2015 and 2019 at the competition and the lack of continuity between different editions made it difficult to have a proper transfer of know-how.

We started working online in distance, since the pandemic restrictions prevented any other type of team working. One of the challenges we encountered was the decision of the dimensions of the aircraft in respect of the regulation geometry, especially for the transportation box' rule, and time constraints, that made our design concept modular, with a particular attention in making the assembly and disassembly as fast as possible. Together with that, we defined an optimized aerodynamic profile to be used and we managed to do many CFD and FEM analyses to prove the validity of our design even before starting the construction. Even though we proceeded slowly in the first period, we managed to carry out a project with solid design choices.

After that difficult period, we began working physically on the construction of the plane, with a big effort in finding sponsors and the right partners that could allow us to build pieces with the appropriate mechanical performance at reasonable prices. This led to the decision of making the main aerodynamic surfaces out of balsa wood and to the design of some 3D-printed parts (such as the cargo bay, the posterior tail joint, the electrical components anterior bay and the cover of the central aluminum joint).

Despite all these critical aspects of the project, we are enjoying this challenge, which offers us the chance to do something beyond what we used to do within standard university courses, giving us the chance of developing and improving our technical skills and our experience within a working team.

All of our work results in a reliable and competitive model, which will be explained in detail in the following pages.

3 Project Management

3.1 Financial Budget

Just from the very beginning of the project, we have focused on finding financial supporters.
We have created social media accounts to gain reliability and, at the same time, we have defined the strategy by offering different sponsorship packages with various benefits according to the support given by the sponsor’s company.

3.1.1 Sponsors relationship

We have offered our sponsors social media visibility, logo space on aircraft surface, team T-shirt and poster.
Partners have supported the project by giving funds, free access to their software to develop the aircraft model, access to their facilities and manufacturing for some parts of the aircraft.
With many sponsors of ours, we have kept in contact throughout the design and test period to give reciprocal continuous feedback. For this support, we are grateful to our sponsors.

Here below is a little presentation of our supporters.

ALTAIR	Altair enhances simulation, improves engineering, optimizes design. Licensing model delivers access to simulation and data analytics technology, enables design and optimization for high performance, innovative, and sustainable products and processes.
Ansys	Ansys is an engineering simulation software to rapidly innovate and easily validate design ideas. Multiphysics simulation gives to Ansys the ability to explore and predict how products will work-or won’t work- in the real world, it is like to be able to see the future.

	Chiloporta is a local online superstore born in 2020 during the pandemic. It delivers groceries and essential goods at home. It helped the sick people who could not go out to buy something.
	Experis is a global leader in IT professional resourcing and managed services. Connecting the power of people and organizations to drive flexible solutions that adapt to evolving technologies and skill demands. Experis helped us to print the 3D parts like cargo bay.
	University of Pisa is currently divided into 20 Departments, with around 150 first and second level degree courses, and several other kinds of postgraduate ones. It cares about its students and supports them during the national and international school competitions.
	Metis 3D lab designs and manufactures special components. It provides 3D printing, CNC machining and laser cutting. Metis 3D printed many parts of the model such main landing gear connection.
	Solidworks develops and markets 3D CAD design software, analysis software and product data management software.

	Pisa utensili provides to its customers the proper special tools very quickly. It cares about its clients, and it makes the possible to satisfy their needs every day.
	EUROAVIA Pisa is a no profit organization based in University of Pisa and affiliate with EUROAVIA, European Aerospace Engineering Students Association. It arranges aerospace meeting, conferences, technical projects, cultural exchanges and social events.
	The Italian association of aeronautics and astronautics (A.I.D.A.A.) is a national non-profit cultural association, recognized as the second oldest scientific aerospace society in the world.

3.2 Time Schedule

Time schedule is a necessary part of every project. It consists in organizing the activity considering the team member’s numbers and skills for all the different field approaches in the project.

3.2.1 Timetable and scheduling

For LeanIng Project, it is important to track and establish a clear road map for every activity assigned to specific sub-teams. Every sub-team submits the updates on the task assigned to the rest of the team periodically during the weekly flight through review. The team leader tracks the progress on a schematic timetable (in the *Figure 3.1* an extract of the table) highlighting the deadlines imposed by regulations and by the design/building scheduled plan.

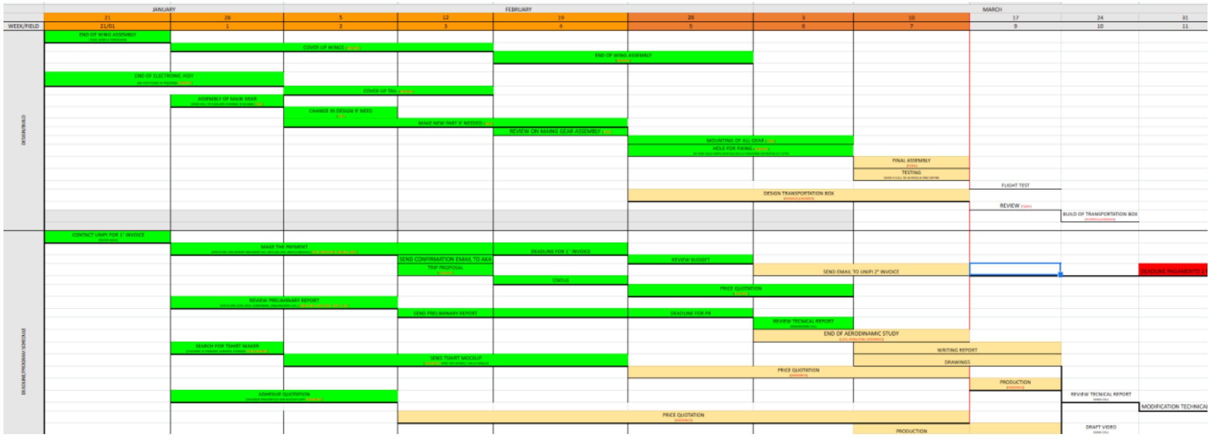

Figure 3.1

The schematic timetable is divided into the task of design/build of the aircraft (e.g., CAD activities, FEM, flight mechanics, the building of a part, etc..) and in task regarding the deadline/program schedule (e.g., sponsors, social, check regulation deadlines and requisites, budget etc). Each task has one or more owners. The task owners are team members specialized in the field of the task.

For the macroscopic time schedule, the approach is the same and follows up on the detailed time scheduling described before. Is the team leader’s responsibility to check this timeline and if necessary, stretch internal deadlines.

4 AERODYNAMIC DESIGN

The aerodynamic design of the model aircraft has been based on the restrained dimensions imposed by the regulations of the competition. As a matter of fact, for the regulations it is mandatory to insert the aircraft inside a square rhombus of fixed dimensions and non-restrained angles.

These restrictions are extremely relevant as far as the aerodynamics and the flight mechanics are concerned because it has been necessary to find a suitable compromise between the wingspan relevant to the aerodynamics and the distance between the wing and the tail relevant to the flight mechanics.

4.1 WING AND TAIL AIRFOILS

The wing airfoil that has been chosen is an optimized one for a Reynolds number of $2{,}5 \times 10^5$. The resultant airfoil has the following characteristics:

- t/c=14%
- Maximum camber of 16% at 20% of the chord

The resultant shape is the one indicated in *Figure 4.1*

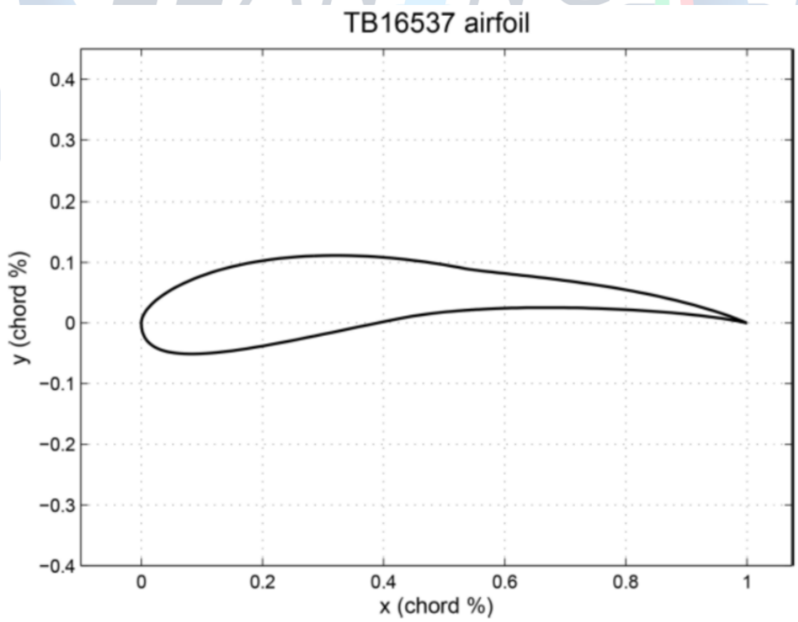

Figure 4.1

From the analysis made by using XFOIL, the characteristic curves shown in *Figure 4.2* have been obtained for the airfoil.

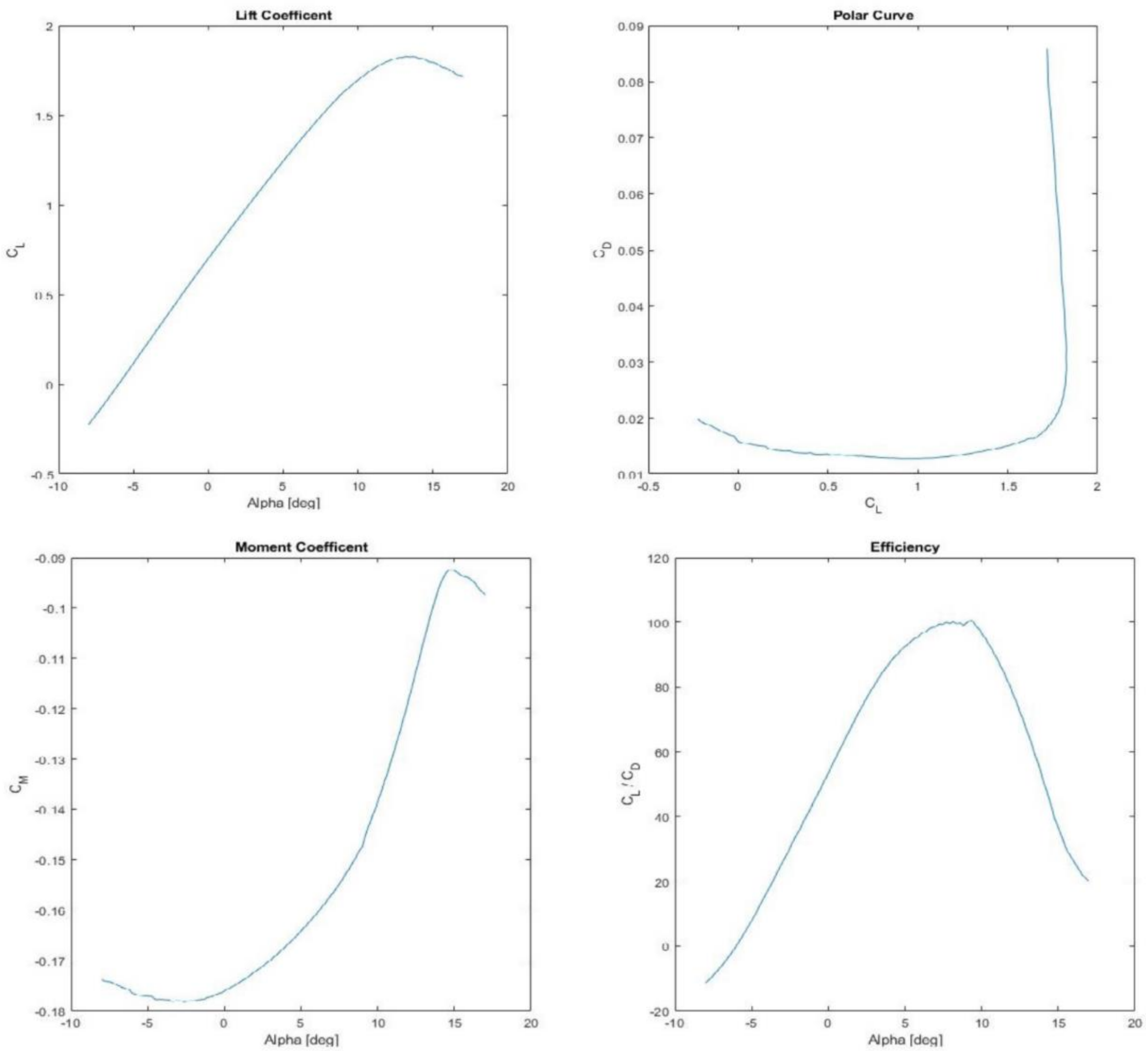

Figure 4.2

Regarding the tail, for both the horizontal and the vertical tail the chosen airfoil has been a NACA 0012.

4.2 Dimensions and Shape of Wing and Tail

The considerations on wing and tail dimensions and shape have been made starting from the restrained dimensions of the model aircraft, which must be inserted in a square rhombus of side 1500 mm and of height 500 mm from the ground, with non-restrained angles between the edges, as shown in *Figure 4.3*.

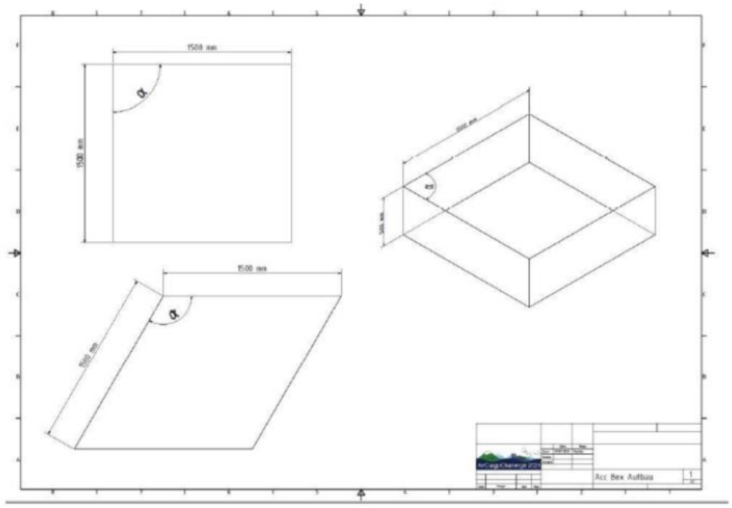

Figure 4.3

4.2.1 Shape and Dimensions of the Wing

For a first approach, a tapered wing had been chosen, with taper ratio λ=0,4 and wingspan 1500 mm. For such a taper ratio, the chord at the root was 250 mm long, whereas the chord at the tips was 100 mm long. The wing design used to include a kink of semi-span of 150 mm, as shown in *Figure 4.4* and in *Figure 4.5*.

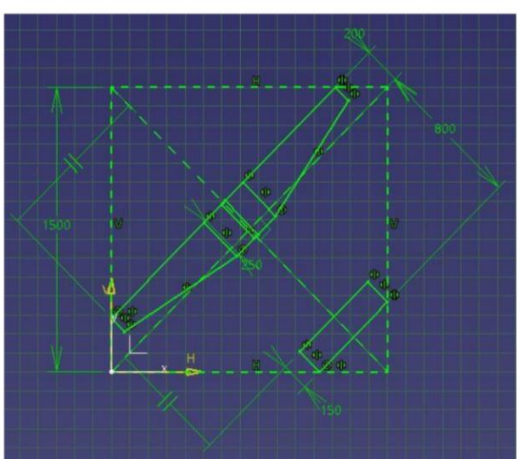

Figure 4.4

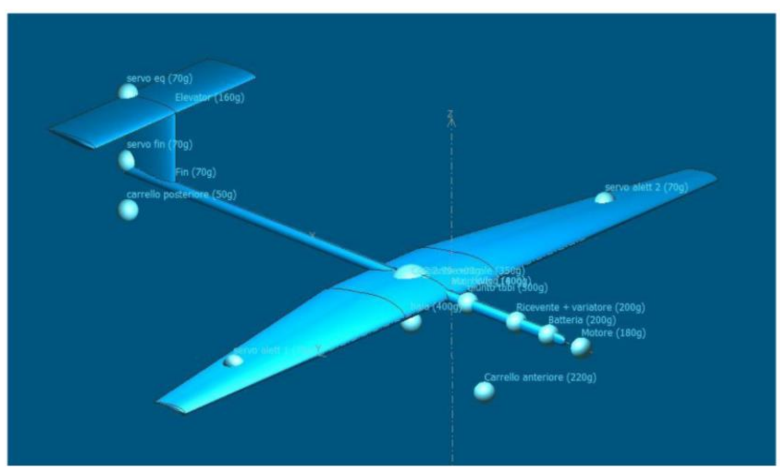

Figure 4.5

For such design, several analyses had been run on XFLR5, where the tapered wing has been coupled with a rectangular T-tail made of symmetrical airfoils, and the results in *Figure 4.6* have been obtained.

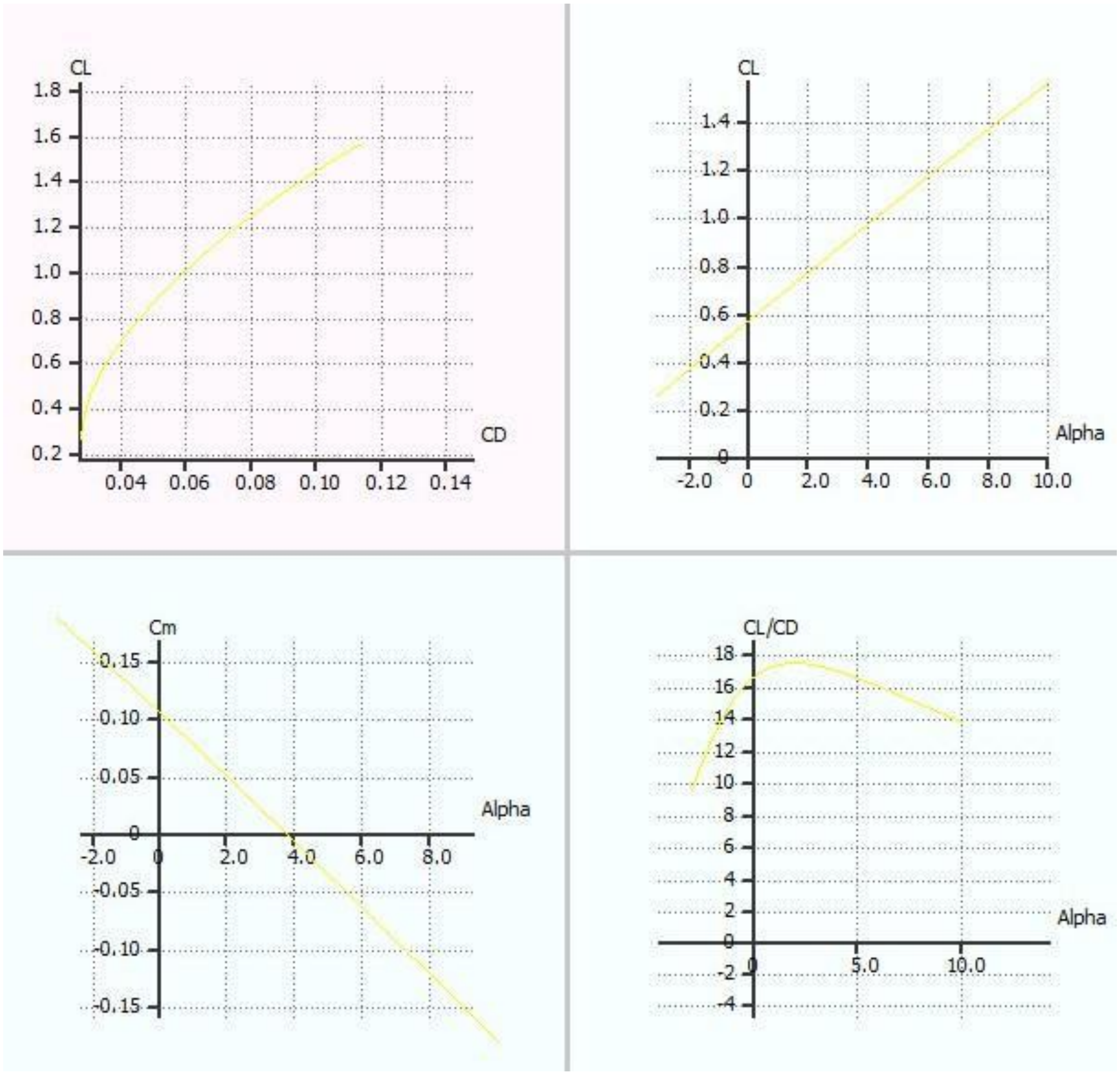

Figure 4.6

Although the results shown by these curves were pretty good, it was soon clear (after the definitions of the weights of some elements of the aircraft) that the amount of lift developed by such a configuration was not enough to balance the load, especially as far as the lift-off was involved.

As a matter of fact, the formula $L = \frac{1}{2}\rho S V^2 C_L$ has been used to calculate the lift of the model aircraft, whereas the formula *L=W* has been used to analyze the equilibrium during the cruise.

From *Figure 4.6* and from the previous formula, it is possible to see that the lift developed by the tapered wing – by considering an ISO atmosphere at h=0 m, a speed of 12 m/s and, a tilt

angle of 2° and an angle of attack of 0°- was around 15,08 N. The choice of considering a cruise speed of 12 m/s has been made to face the worst case ever, because the expected speed is of 15 m/s.
To have a cruise equilibrium condition (L=W), it would have been necessary not to exceed the mass of 1,54 kg for the aircraft, payload included.
Such a value was definitely too restricted to reach and would have affected the design of the aircraft in a negative way. Moreover, there would have been a very heavy restriction on the payload to carry during the competition, so an alternative configuration has been developed. As a matter of fact, to reach acceptable amounts of loads with this configuration a too extreme angle of attack would have been necessary, making the model likely face the risk of stall, especially during take-off.
In order to increase the amount of lift developed by the wing and, consequently, the load allowed, it has been chosen to redesign the whole wing by turning its tapered shape into a rectangular one.
The results of the analysis made with XFLR5 on the whole aircraft with the rectangular wing and the rectangular T-tail are those shown in *Figure 4.7*.

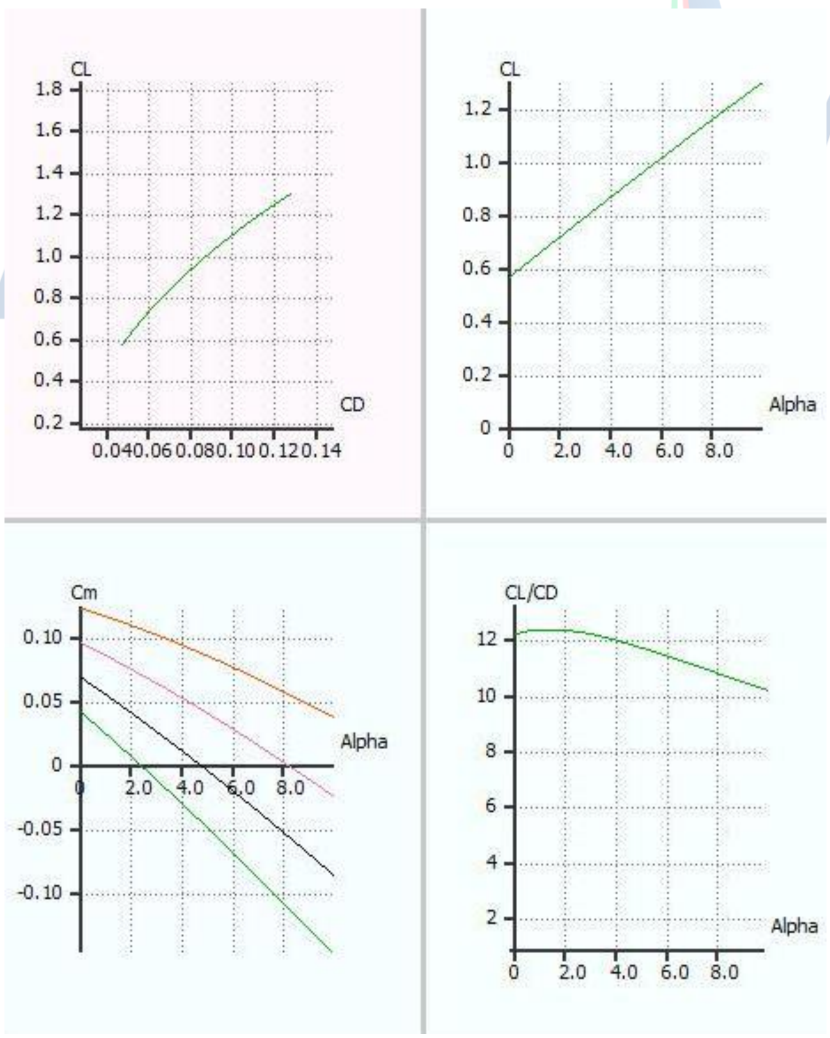

Figure 4.7

As shown in *Figure 4.7*, the rectangular shape is quite penalizing in terms of $C_{L\alpha}$, since the slope of the C_L-α curve is lower than for the tapered wing. Anyway, the equation seen before $L = \frac{1}{2}\rho S V^2 C_L = \frac{1}{2}\rho S V^2 C_{L\alpha}\alpha$ depends both on the slope and on the area, but, since the increase of area is greater than the decrease of slope, the rectangular shape develops a bigger amount of lift for equal conditions. Moreover, the wingspan has been increased until 1836 mm by changing the distance between wing and tail, as long as the flight mechanics has allowed it, as shown in *Figure 4.8*.

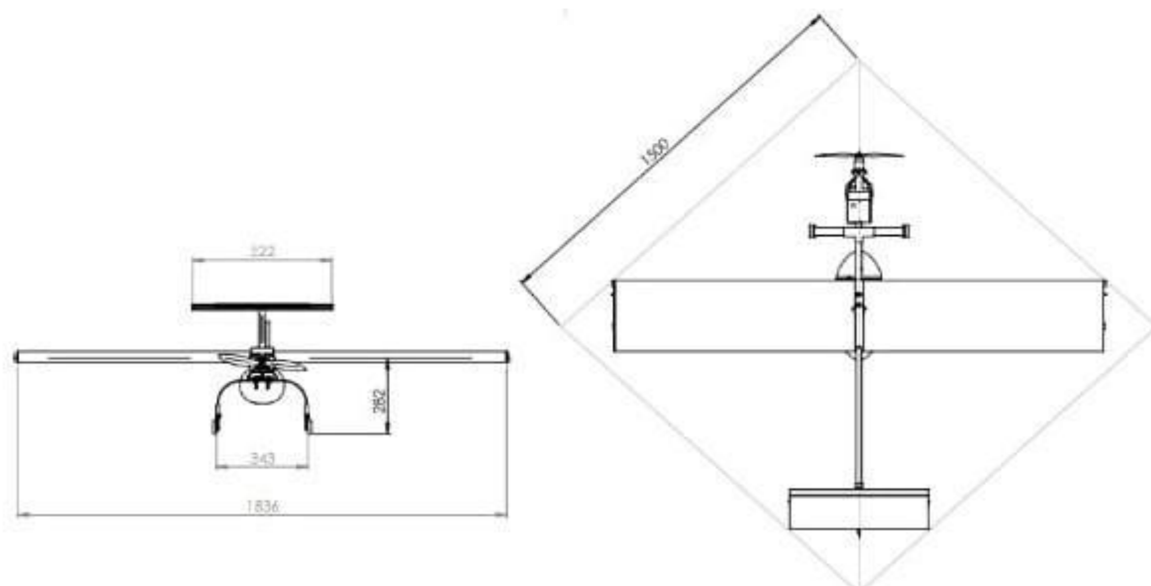

Figure 4.8

For such a wingspan, the value of developed lift has become around 24,3 N, by considering an ISO atmosphere at h=0 m, a cruise speed of 12 m/s, a tilt angle of 2° and an angle of attack of 0°. This value, even if it is greater than the previous one, is still not sufficient, so a more suitable angle of attack has been researched.
To find the angle of attack for the cruise, the following equations have been used:

- $L = \frac{1}{2}\rho S V^2 C_L = \frac{1}{2}\rho S V^2 C_{L\alpha}\alpha$
- $L = W$

The load has been chosen by considering a mass of the aircraft around 3800 g and a payload of 1200 g, so a lift of 49 N is necessary. For the previous conditions of air and speed, the resultant lift coefficient is C_L=1,2, so the resultant angle of attack is around 8°, as shown by the curves in *Figure 4.7*. Obviously, this is a very conservative estimate in terms of speed, whereas, for the expected speed 15 m/s, the resultant C_L is around 0,77 and the angle of attack is around 3°.
Actually, the rectangular shape is way less effective than the tapered one as far as the vorticity is concerned and winglets or rounded tips may be needed. Due to the very low speed of the aircraft and the complexity of the design of winglets, it has not been considered as necessary to design them. A second option to reduce the longitudinal vorticity consists in rounded tips. For this reason, two different models of the wing have been developed on Solidworks, in order to

analyze them both through CFD analyses and to compare the results, especially regarding the drag.
The analyses have been done on the couple wing-tail, using the same tail for both cases (T-tail), but two different wings.
The two wings have the same dimensions and shape except for the tips, which are rounded tips in one case and simply cut tips in the other one.
For the two analyses Ansys Fluent has been used and two different flight conditions have been studied for each configuration (take-off and cruise).
For the take-off, the flight conditions were the following:

- Speed: 15 m/s;
- Angle of attack: 7°.

For the cruise, the flight conditions were the following:

- Speed: 15 m/s;
- Angle of attack: 3°.

For both the conditions and the configurations a tilt angle of 2° has been considered for the wing. The results obtained by the CFD analyses are those explained in *Table 4.1*.

Configuration	Mission Phase	Angle of Attack	Speed	Lift (L)	Lift Coefficient (C_L)	Drag (D)	Drag Coefficient (C_D)
Simply Cut Tips	Take-off	7°	15 m/s	80,1 N	1,17	6,7 N	0,098
Rounded Tips	Take-off	7°	15 m/s	76,5 N	1,12	6,4 N	0,094
Simply Cut Tips	Cruise	3°	15 m/s	58,8 N	0,86	4,4 N	0,064
Rounded Tips	Cruise	3°	15 m/s	56,0 N	0,82	4,1 N	0,061

Table 4.1

As it can be seen from the table, the rounded tips haven't reduced the drag enough to be considered much advantageous, but they have instead reduced the lift of a non-negligible amount. For this reason, the rectangular wing with simply cut tips has been chosen.
As a verification, CFD analyses have been made on the definitive configuration of the couple wing-tail even for a lower speed of 12 m/s to be sure of developing a sufficient amount of lift both during take-off and during cruise. The results are those shown in *Table 4.2*.

Mission Phase	Angle of Attack	Speed	Lift (L)	Lift Coefficient (C_L)	Drag (D)	Drag Coefficient (C_D)
Take-off	7°	12 m/s	50,8 N	1,17	4,3 N	0,098
Cruise	3°	12 m/s	37,1 N	0,86	2,8 N	0,064

Table 4.2

From these simulations, it is quite evident that a speed of 12 m/s is a limit case which should not be reached, because the lift developed is too low for the expected payload.

In conclusion, for a last validation, CFD analyses have been done on the whole model, as shown in *Figure 4.9*, in two different configurations at two different speeds:

- Take off:
  - Angle of attack 7° and speed 12 m/s
  - Angle of attack 7° and speed 15 m/s
- Cruise:
  - Angle of attack 3° and speed 12 m/s
  - Angle of attack 3° and speed 15 m/s

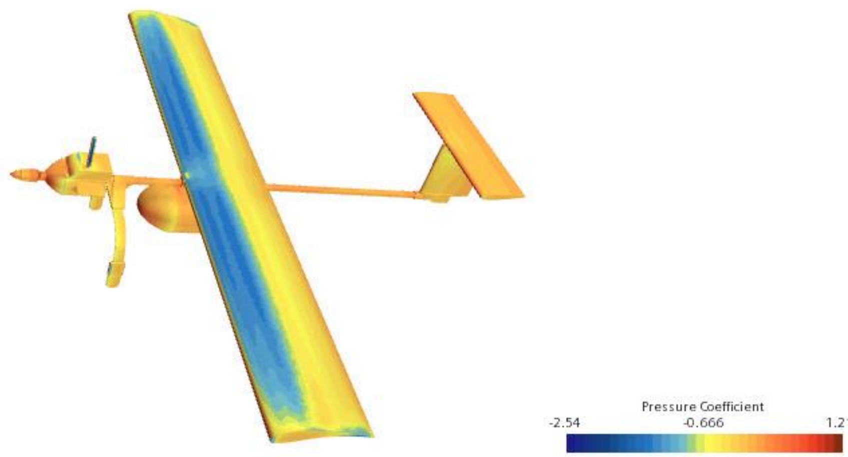

Figure 4.9

For these conditions, the results shown in *Table 4.3* have been obtained.

Mission Phase	Angle of Attack	Speed	Lift (L)	Lift Coefficient (C_L)	Drag (D)	Drag Coefficient (C_D)
Take-off	7°	12 m/s	51,42 N	1,27	5,89 N	0,15
Cruise	3°	12 m/s	38,38 N	0,95	4,22 N	0,14
Take-off	7°	15 m/s	81,30 N	1,29	9,14 N	0,15
Cruise	3°	15 m/s	60,65 N	0,96	6,52 N	0,10

Table 4.3

As shown by *Table 4.3*, the results are very similar to those obtained analytically by using the curves from XFLR5 as long as small angles of attack are concerned, whereas they tend to differ when the angle of attack increases.

Finally, the results obtained by the CFD analyses on the whole model are similar to those obtained by only considering the wing and the tail and it has been confirmed that a speed of 15 m/s would be desirable to reach the necessary amount of lift, whereas a speed of 12 m/s would be too penalizing. Anyway, a speed of 12 m/s is a very low value that has been considered only for the sake of being conservative and cautious.

4.2.2 Shape and Dimensions of the Tail

For the tail, three different configurations have been considered: a V-tail, a T-tail and a standard tail.
These three configurations have been analyzed through XFLR5 in order to find the one minimizing the downwash effect from the wing, as shown in *Figure 4.10*.

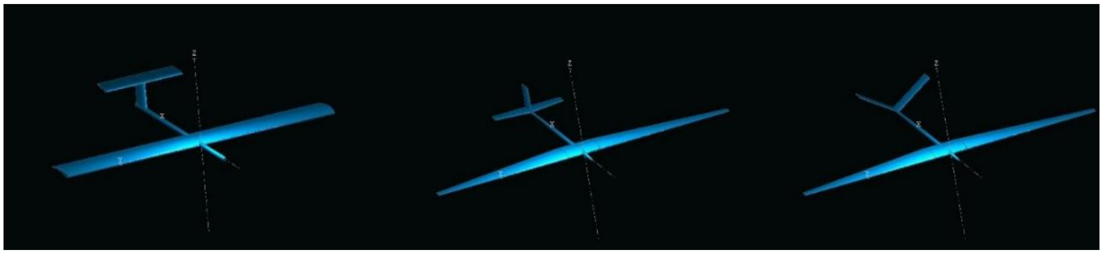

Figure 4.10

The winning configuration is the T-tail, since it is the least influenced one by the wake of the wing thanks to its elevated position.
The in-plan shape of the tail is a rectangular one, with a span of 522 mm and a chord of 150 mm.
Furthermore, for flight mechanics reasons the tail has a tilt angle of -4° with respect to the fuselage. For further considerations about the flight mechanics, there's a dedicated chapter.

4.3 CARGO BAY

For the cargo bay, an asymmetrical ogive shape has been chosen to be as aerodynamic as possible. The choice of an asymmetrical bay comes from the need for an aerodynamic shape at the least weight possible. As a matter of fact, the bay is elongated at the back in order to reduce the wake, whereas the front is shorter to limit the use of material and, consequently, the weight of the whole bay.
To reach the best-fit shape, some CFD analyses have been done, as shown in *Figure 4.11*.

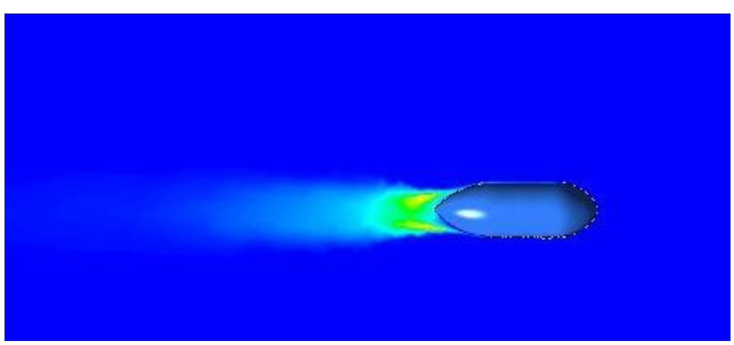

Figure 4.11

5 STRUCTURES

The present chapter describes the features and functionality of the main structures and joints used in the development of our model, along with their production technology and mechanical strength.
It is divided into four sections, regarding the wing, the “fuselage” and the central joint, both horizontal and vertical tail and the cargo bay.

5.1 WING

The rectangular planform of the wing was made by using a Balsa Wood shell, reinforced with longitudinal and transversal stiffening elements. As show in the following image, the main longitudinal elements consist of:

- A tubular section (1), made of composite materials (carbon/epoxy), which extends for about 1/3 of the wingspan from the root section and represents the “pivot” point of each half-wing.
- A main wood spar (2), placed in the proximity of the leading edge which extends for the entire wingspan length.
- Two smaller spars (3) placed in correspondence of the aileron-dedicated surface
- A leading-edge longitudinal element (4), which provides an additional support for the transversal ribs.

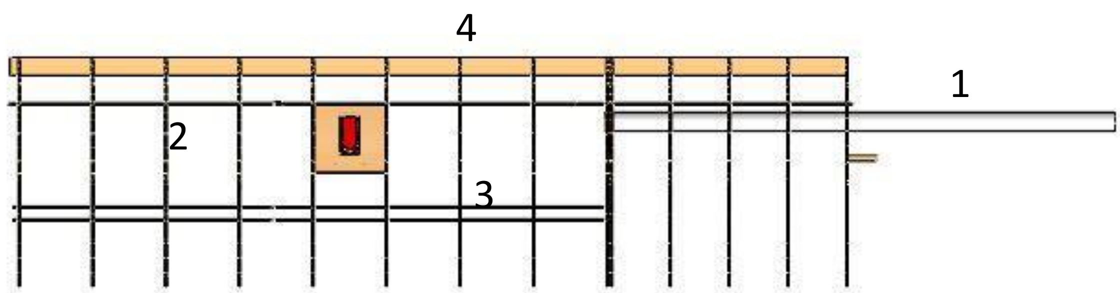

The transversal elements (5) consist of wood ribs. We have chosen two different spacings for the inboard and the outboard half-wing, with a “separation” section in correspondence of the aileron breaking section, where we have decided to place two ribs very close to each other.
Additional reinforcing wood elements (6) are used between the ribs to ensure the compliance of the desired stiffness of the wing as a whole.
Both longitudinal and transversal elements were made by laser cutting, starting from the CAD drawing.

5

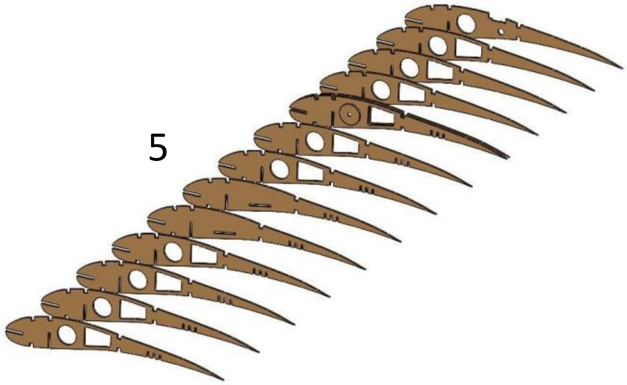

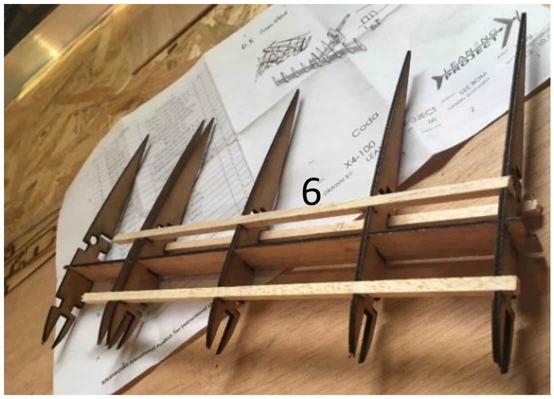

The different components of the structure are kept in contact using notches and epoxy adhesive.

Many finite elements analyses have been performed to estimate stresses and strains and therefore ensure the respect of stress and displacement limitations:

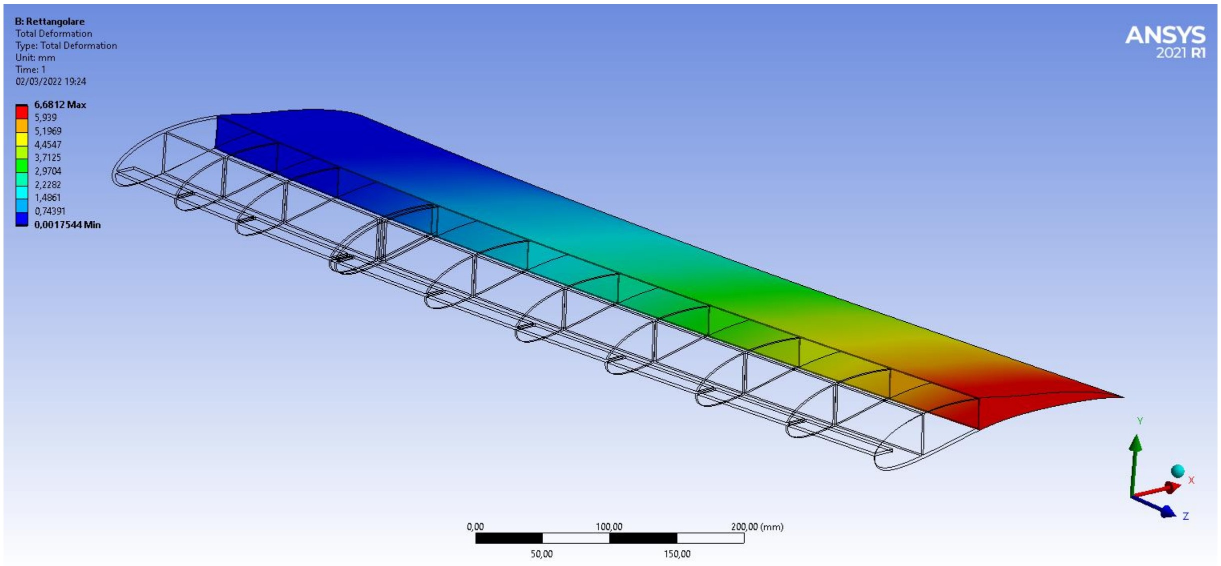

5.2 "FUSELAGE" AND CENTRAL JOINT

The so-called "fuselage" of the model consists of a carbon/epoxy tube beam, split into two parts in order to respect the constraint on the maximum dimension of the transportation box. The two sections of the tube have an internal diameter of 16 mm and an external diameter of 20 mm and they are connected together by a double joint. This joint consists of two parts: an internal aluminum tube (1) and an external Teflon attachment (2):

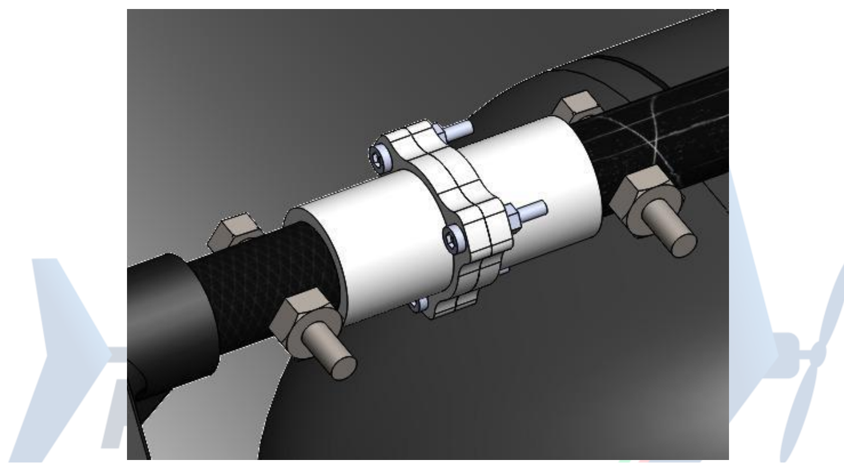

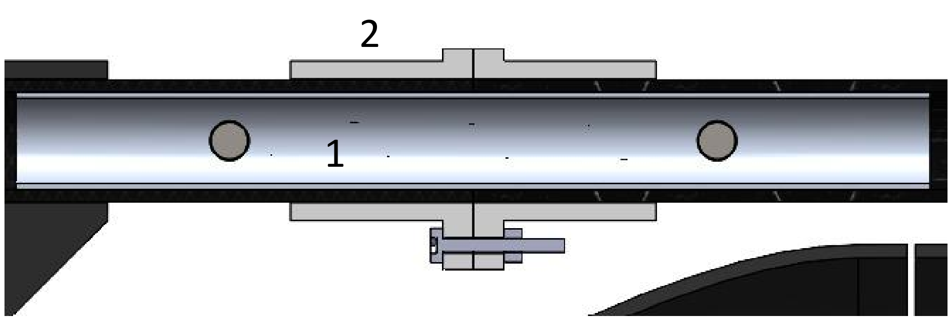

The internal tube is fastened to the two sections of fuselage by using M6 bolts, while the external parts are mounted with interference on the carbon tubes and then connected by means of M3 screws. This type of joint has proved to be very effective in transferring the driving force of the engine to the rest of the model and to inhibit relative rotations between the two sections of fuselage.
A central aluminum joint is also used to create the intersection between the fuselage and the wing. This joint has been made starting from a solid aluminum block and machined to its final shape:

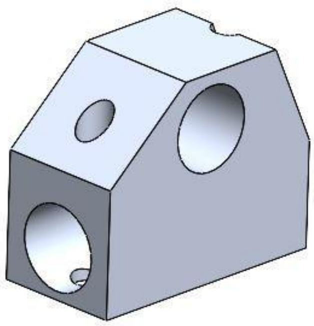

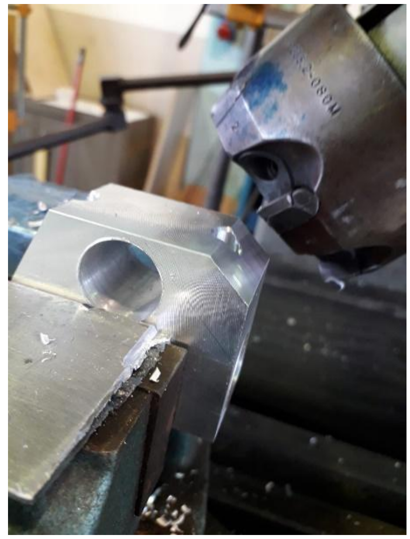

This joint has been "covered" by a 3D printed plastic fairing, to ensure continuity with the wing airfoil. The fairing is connected to the joint and the tube using M6 bolts.

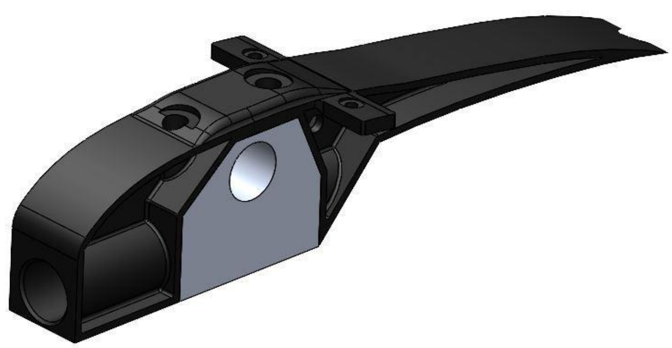

The central joint also provides the point of attachment of the two half-wings to the rest of the model, by means of two M4 screws that go right into the corresponding drive-in nuts placed inside the structure of the wing.

5.3 Horizontal and vertical tail

The structure of the horizontal and vertical tail is very similar to the one of the wing.
As matter of fact, these surfaces consist of a thin wood shell reinforced with longitudinal and transversal elements.

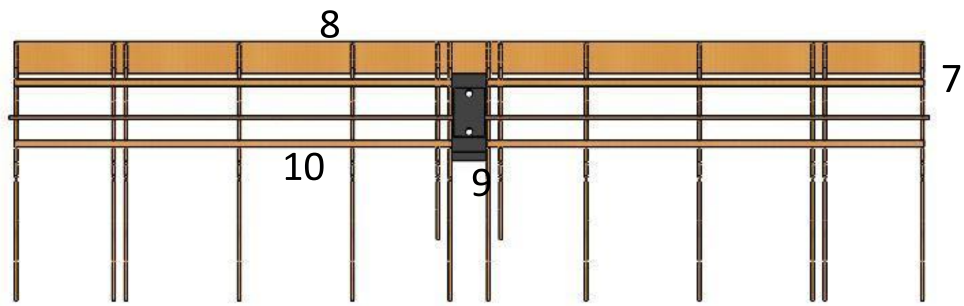

There are one main spar (7) and four other stiffening and stabilizing longitudinal elements (10). In addition, the leading-edge element (8) provides more stability to the ribs. The number 9 is a 3D printed connection plate that we have used to join the horizontal to the vertical surface by means of two M4 screws, as shown in the following image:

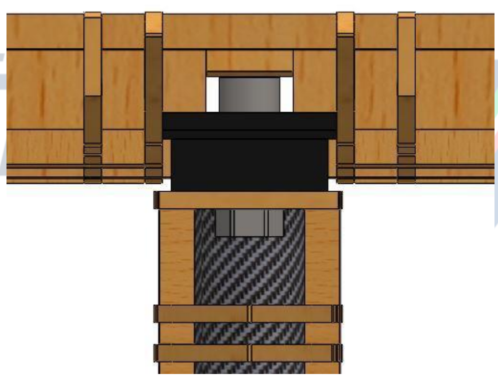

The vertical tail contains almost the same elements of the horizontal tail with the exception of a main composite spar instead of a wood one.

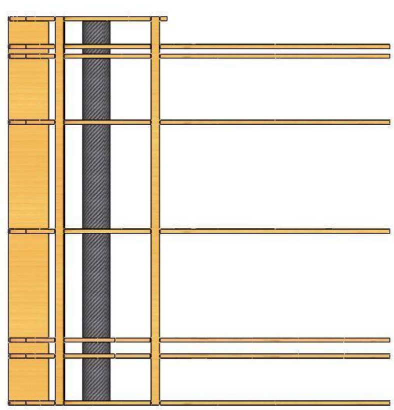

This composite spar has a tubular cross section and this choice is related to our concern about a correct load transfer from the horizontal to the vertical surface. In addition to that, the tubular section provides a safe path to the electronic wiring of the elevator servos.
The whole tail complex is connected to fuselage tube using a 3D printed plastic joint and a M6 bolt:

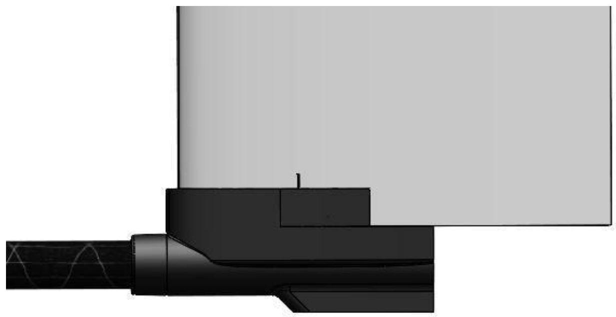

As we did for the wing, we have analyzed the tail structures using a finite elements solver to check the maximum displacements and the maximum stresses. An example is shown in the following image:

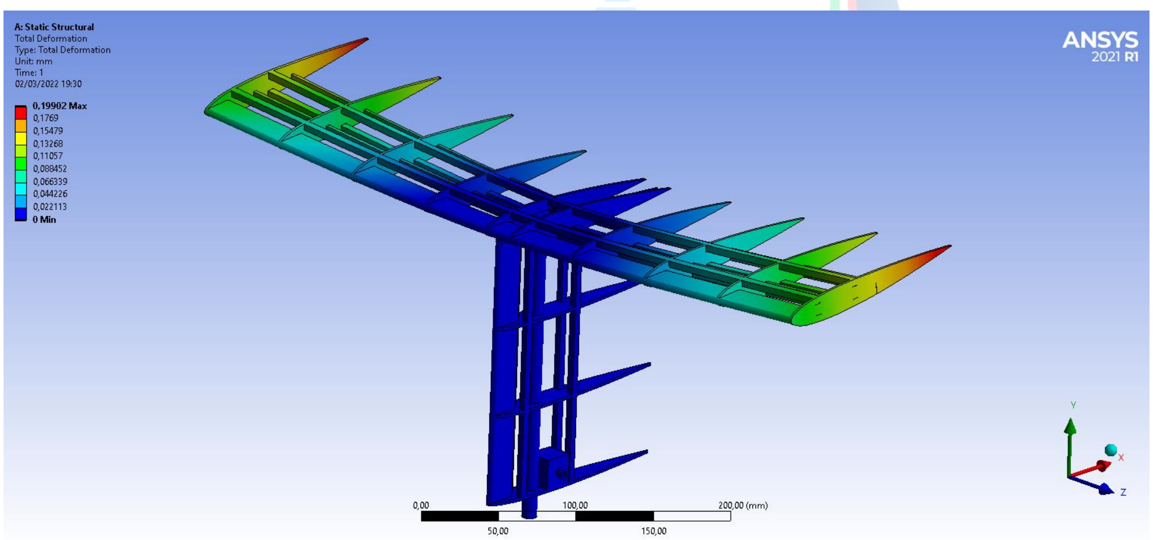

5.4 CARGO BAY

The cargo bay has been made by assembling three different parts: the central cylindrical region (that contains the payload) and the two (front and rear) fairings, that also represent the openings necessary for load and unload of the payload and electrical components.

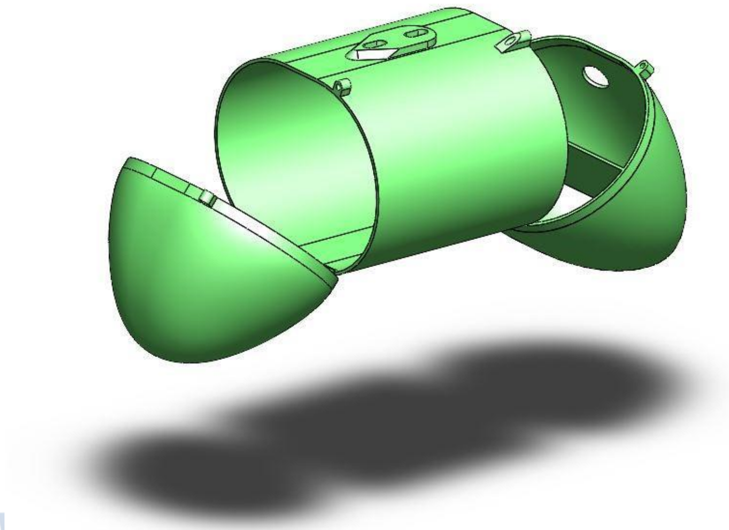

These parts are made by 3D printing of plastic, reinforced with Kevlar fibers. The choice of Kevlar instead of Carbon fibers has been made because we needed the bay shell to be "transparent" to the electro-magnetic radiation. The fairings are connected to the central part with four hinges (two for each side) that allow the relative rotation.



The whole bay assembly is attached to the central joint described in section 5.2 with the same two M6 bolts that pass through the fuselage tube. For this reason, a region of increased thickness is present in correspondence of the joint location. A horizontal "shelf" has been designed to accommodate the servos battery and the receiver in the back of the bay. A circular hole realized in the top of the rear fairing allows the passage of the wires.

6 FLIGHT MECHANICS

The basic theoretical scheme used to study the longitudinal equilibrium and stability of our model is the simple "beam" scheme, shown in the figure below:

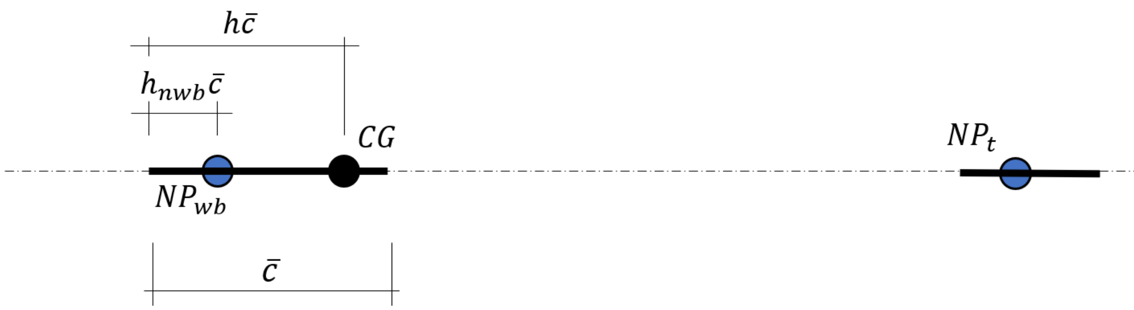

The length $\bar{c}$ is the mean aerodynamic chord of the wing (equal to 250 mm) while NP_{wb} and NP_t are the neutral points of the wing-body system and the horizontal tail. For the sake of simplicity, we assume that the horizontal surface of the tail is placed at the same vertical coordinate of the wing. The CG point is the position of the center of gravity. The location of these points is expressed in terms of $\bar{c}$ and an adimensional coefficient h or h_{nwb}. The aerodynamic, inertial and propulsive forces are applied as shown in the next figure:

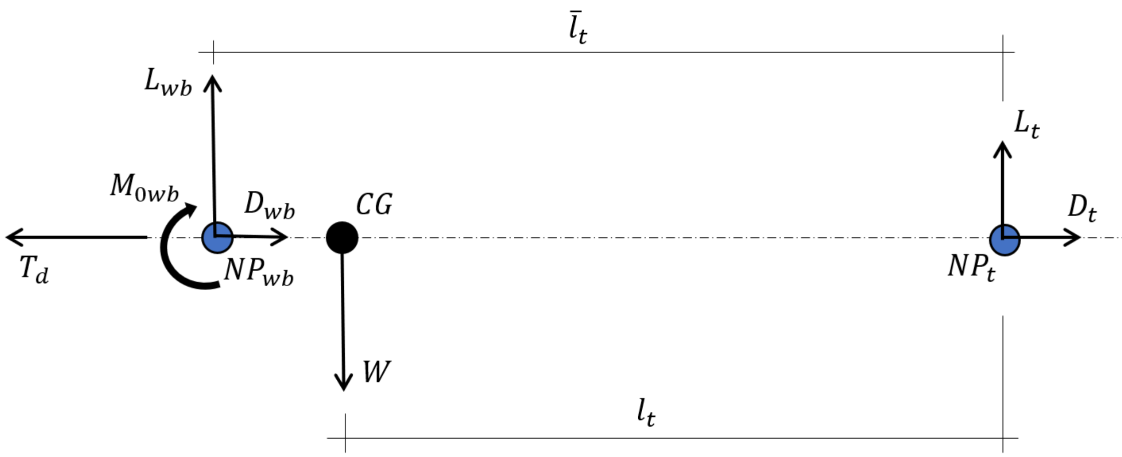

For the equilibrium of forces and moment, the following equations must be satisfied:

$$T_d = D_{wb} + D_t$$

$$W = L_{wb} + L_t$$

$$M_{0wb} + L_{wb}(h - h_{nwb})\bar{c} - L_t l_t = 0$$

This scheme will be further simplified by considering the overall neutral point of the aircraft, NP, and his position, located by the adimensional coefficient h_n:

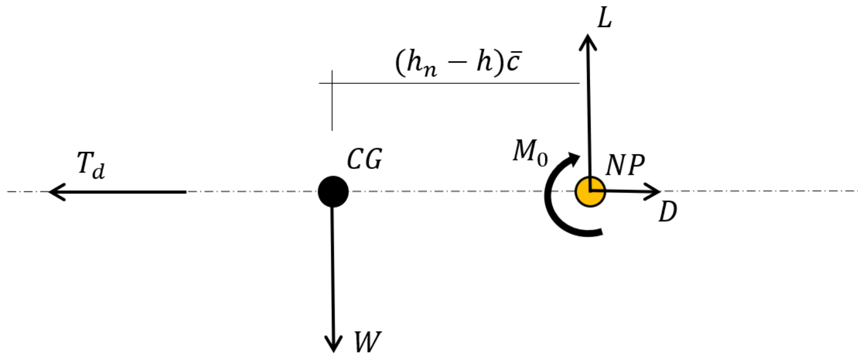

The total lift and drag, L and D, are applied in NP and M_0 is the zero-lift total aerodynamic moment calculated with respect to NP:

$$L = L_{wb} + L_t = W$$

$$D = D_{wb} + D_t = T_d$$

$$M_0 = M_{0wb} + L_{wb}\overline{l_t} = L(h_n - h)\bar{c}$$

where the quantity $(h_n - h)\bar{c}$ must be greater than 0.
To calculate the position of the neutral point and to draw the characteristic curves of the airplane, the software XFLR5 has been used. The main results of the analyses are presented in the following sections.

6.1 THE MODEL

Firstly, a 3D model of the complete airplane is created: the airfoils used for the wing and tail are the TB16537 and the NACA0012, already analyzed in the aerodynamics sections.

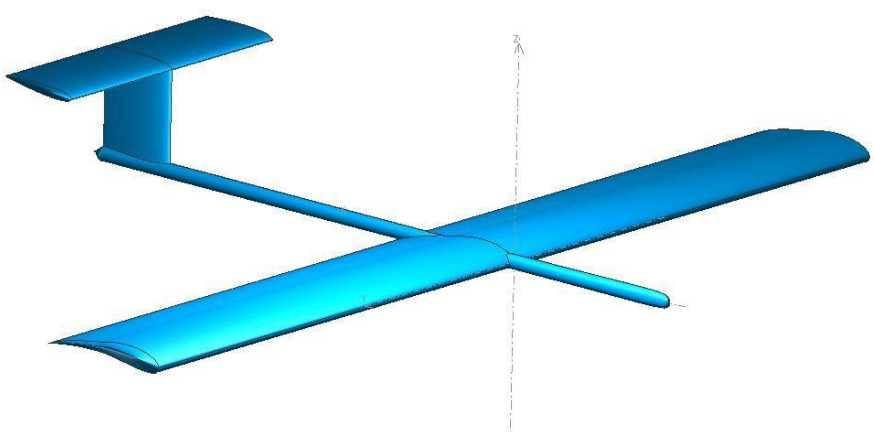

Then the masses have been assigned to the lifting surfaces, to the fuselage tube and to the concentrated loads like engine and propeller, landing gears, servos, cargo bay, payload and others:

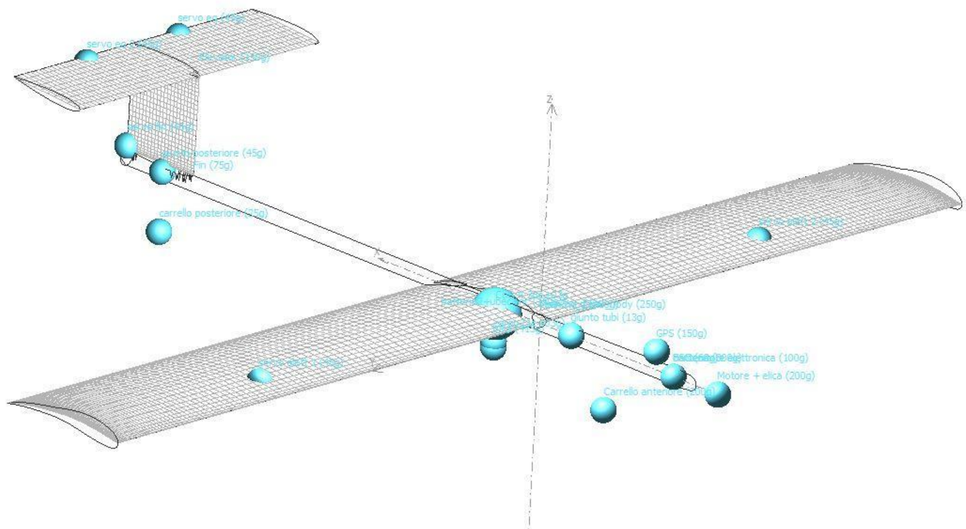

Finally, the panel mesh has been created on the lifting surfaces.

6.2 Analysis and Results

A fixed speed, ring vortex (VLM2) viscous analysis has been performed. We have taken as a reference a velocity of 12 m/s. An interval of angles of attack going from 0 to 10 degrees with increments of 0,15 degrees has been considered to draw the characteristic curves of the model. We have managed the design in order to make the CG of the cargo bay coincident with the CG of the model. In this way, the payload in the nominal position doesn't affect the position of the CG. The nominal position of the payload is set to be at about 10 cm from the leading edge of the wing. To assess the sensitivity of the airplane stability to the payload position we performed the analyses also for the position of the payload of 5 cm and 15 cm from the leading edge.

6.2.1 C_L - C_D curve

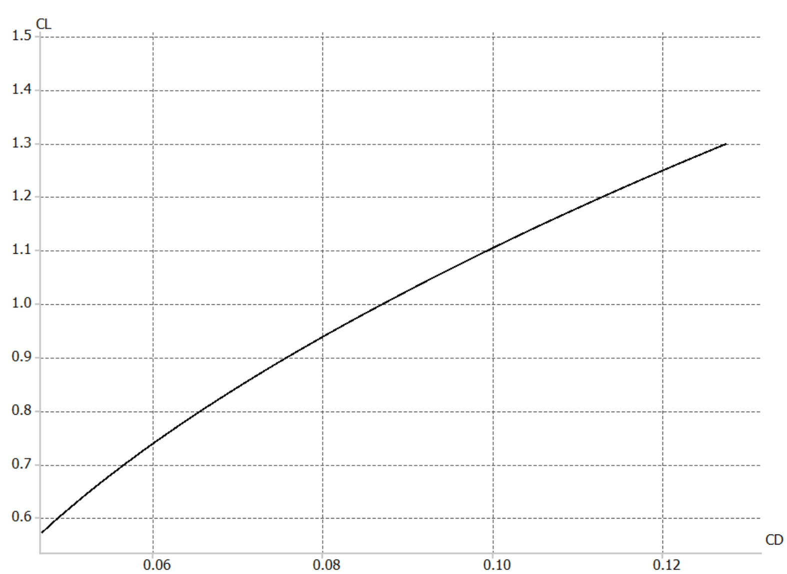

6.2.2 C_L - α curve

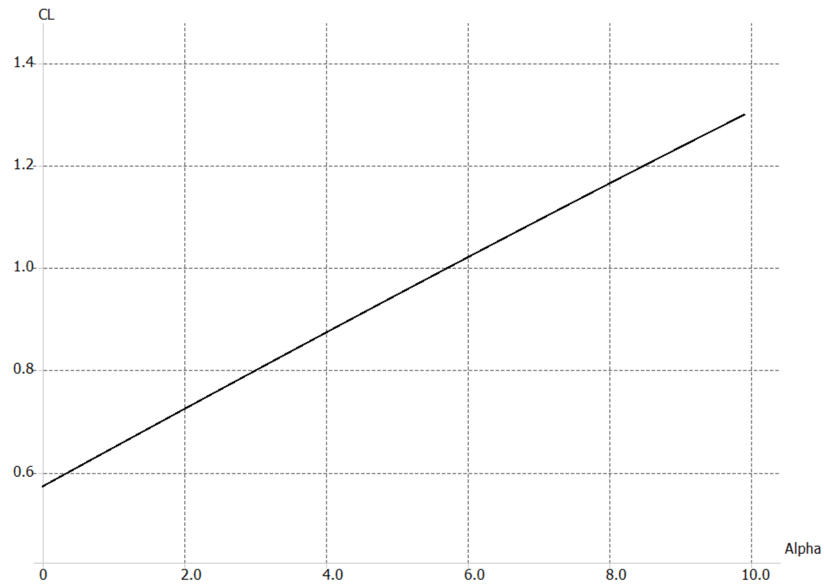

6.2.3 C_m - α curve

We have done three stability analyses for the payload positions of 5 cm, 10 cm (nominal) and 15 cm from the leading edge of the wing, considering a payload of 1 kg. The relative curves of the pitching moment coefficient are shown below:

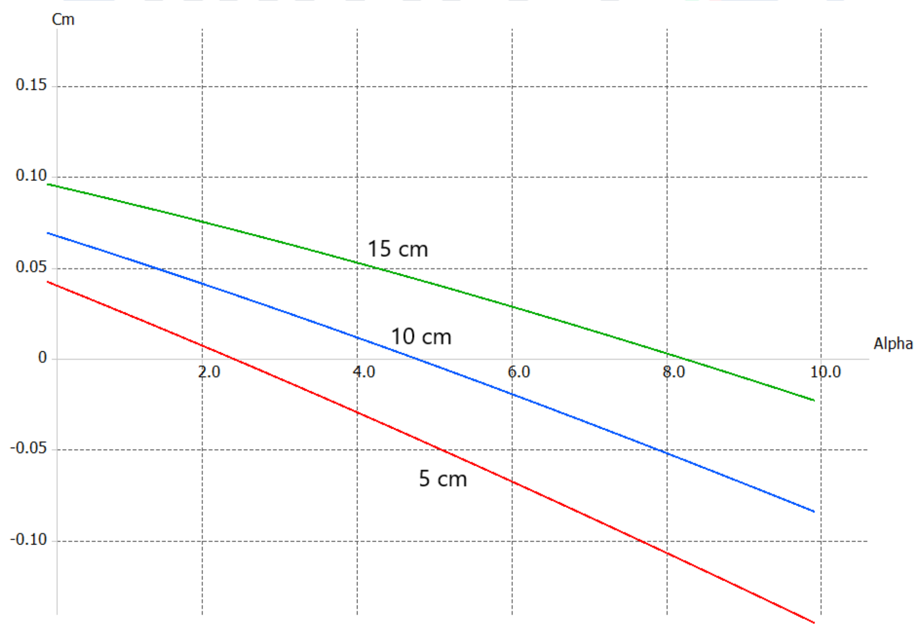

The stability margin of the aircraft has been calculated by:

$$SM = h_n - h$$

where h_n and h are those defined previously.

The stability margins for the three positions of the CG are then:

$$SM_5 = 0{,}24$$

$$SM_{10} = 0{,}19$$

$$SM_{15} = 0{,}15$$

7 PAYLOAD PREDICTION

The payload prediction has been a topic of great concern in the first part of the design of the aircraft. In the first place we used the formula below:

$$M_{payload} = \left(\frac{v^2 S C_{L\,cruise}}{2g}\right)\rho - M_{aircraft}$$

Which is in accordance with the given formula:

$$Predicted\ payload\ [kg] = a \cdot air\ density\ \left[\frac{kg}{m^3}\right] + b$$

With: $a = \left(\frac{v^2 S C_{L\,cruise}}{2g}\right) = 4{,}062\ m^3$ and $b = -M_{aircraft} = -3{,}8\ kg$

Where:

- v = cruise velocity $= 15\ \frac{m}{s}$
- $C_{L\,cruise}$ = Lift coefficient at cruise incidence $= 0{,}77$
- $S =$ wing area $= 0{,}46\ m^2$
- $g =$ gravitational acceleration $= 9{,}81\ \frac{m}{s^2}$
- $\rho =$ air density $= 1{,}225\ \frac{kg}{m^3}$
- $M_{aircraft} =$ mass of the aircraft without the payload

Using all these data the resulting predicted payload is about 1,2 kg (the equivalent of 4 blood bags). After the designing phase we have proceeded with the CFD analyses, which confirmed all our expectations on the maximum weight we can carry.
Though we used the air density at sea level (ISA convention) for the calculation, we knew that air density could vary with altitude and weather conditions, so we have done a brief study on the variability of the maximum payload with the variation of the air density. The range we have chosen for the air density is from 1 kg/m³ to 1,4 kg/m³ because we have estimated this as the more realistic one considering the possible variation of pressure, temperature and humidity during the period of the competition.

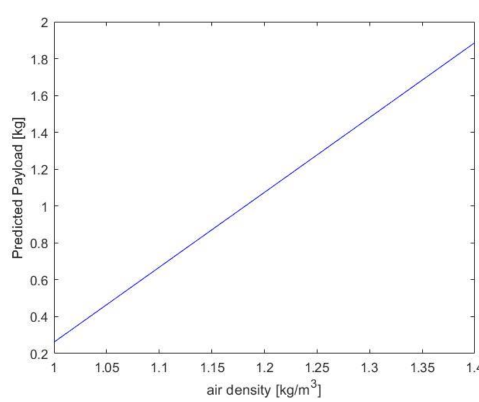

Figure 7.1 variation of the predicted payload with the air density.

8 Outlook

As you may have witnessed in the previous pages, we have made a huge effort to assure that our airplane could be competitive in the Air Cargo Challenge 2022 and we have given our best to achieve such a result in terms of teamwork, design and, most importantly, problem solving. We have faced many challenges during the process of construction and testing of the airplane, but by cooperating and bringing all our knowledge and skills together we have managed to turn our project and ideas into something real and concrete, which hopefully will allow us to reach good results in the upcoming competition.

Furthermore, we'd like to thank our pilot and mentor Gerardo Dello Ioio, who has been fundamental for the development of the project and for the testing phase; he has given us his time and experience in dynamic modeling, permitting us to achieve our final result; we would also like to thank professors G. Lombardi and M. Maganzi for all the technical support and for all the resources they have made available to us.

We must not forget that the entire work wouldn't have been possible without all our sponsors:

- Metis 3D Lab
- Solidworks
- Ansys
- AIDAA
- Experis
- PiÙ
- Chiloporta
- Centro Stampa Faccini
- Altair

and the economic support by our university.

All our gratitude goes to EUROAVIA and Aka Modell Munich that have given us the opportunity to participate in this competition which allows students from all over Europe to implement what they study in a competitive but fair environment.

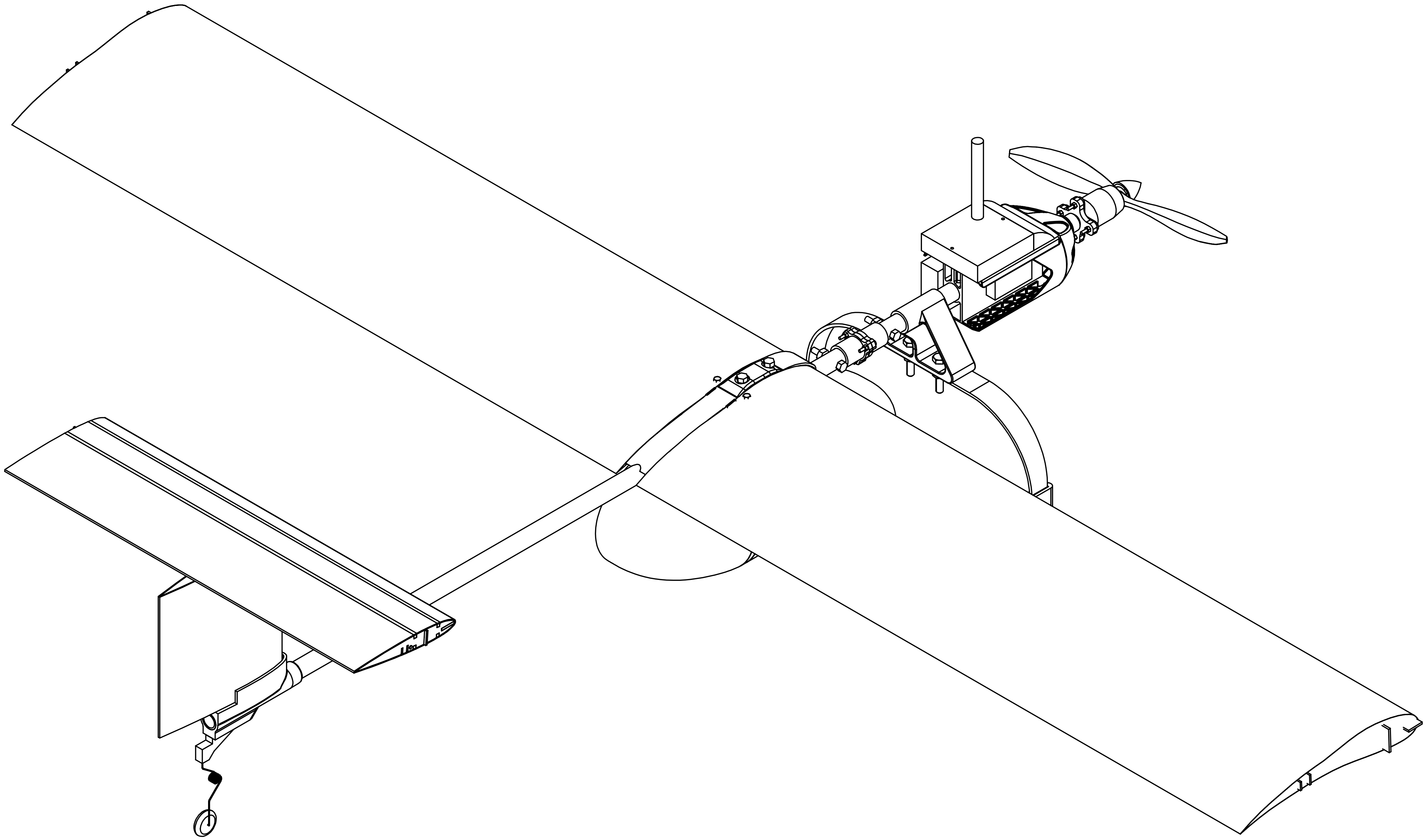

TITLE:	LP1 ISOMETRIC PERSPECTIVE
CODE:	LP1_01
DRAWN BY:	LEANING PROJECT
SCALE:1:5	REV: 01
	SHEET 1 OF 1

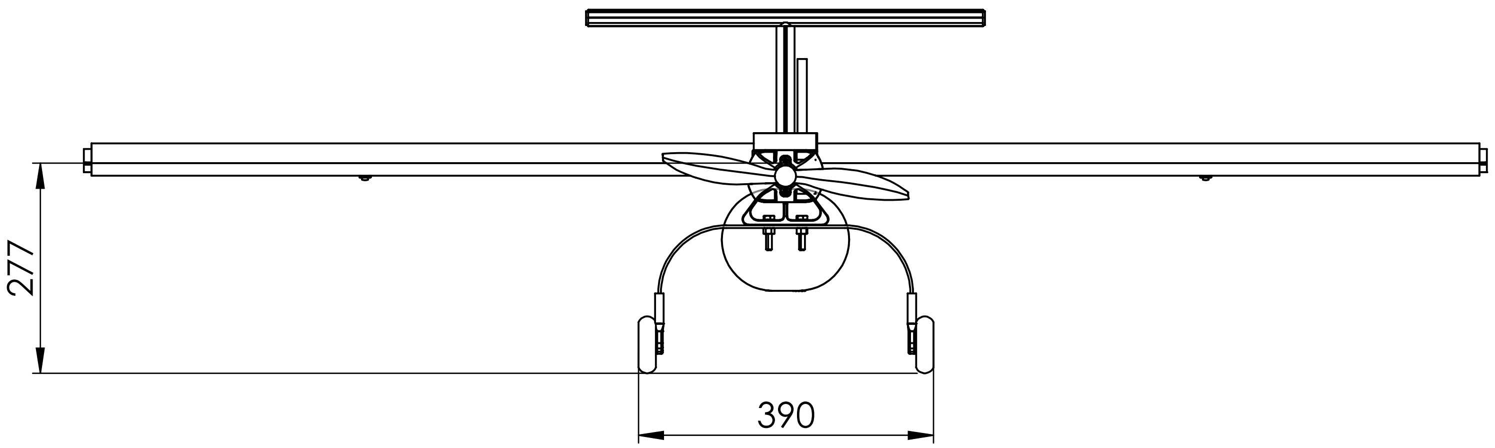

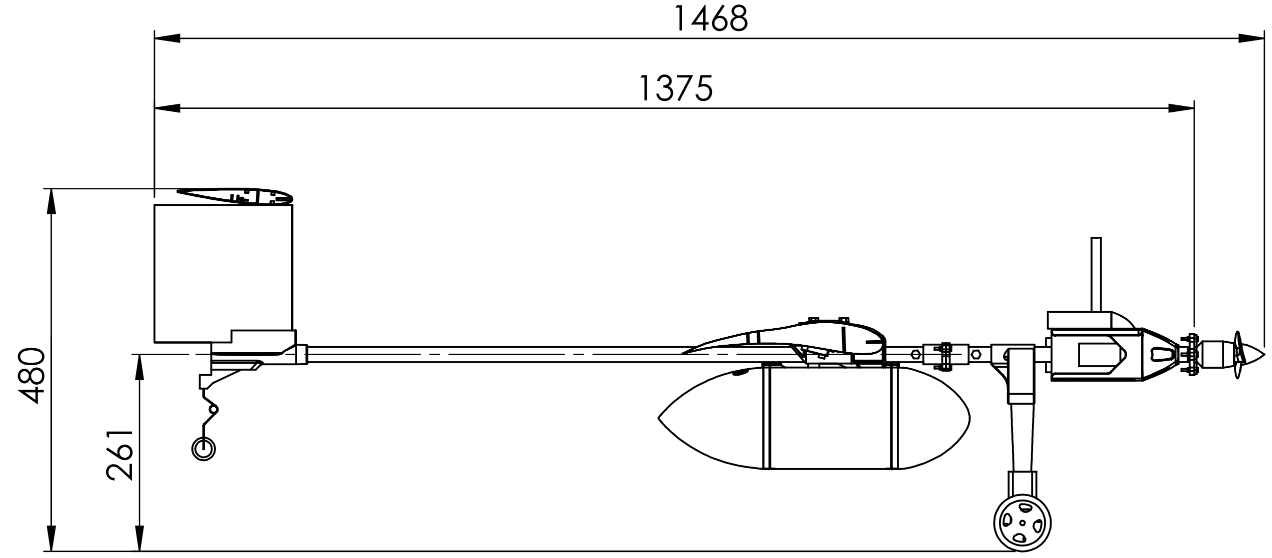

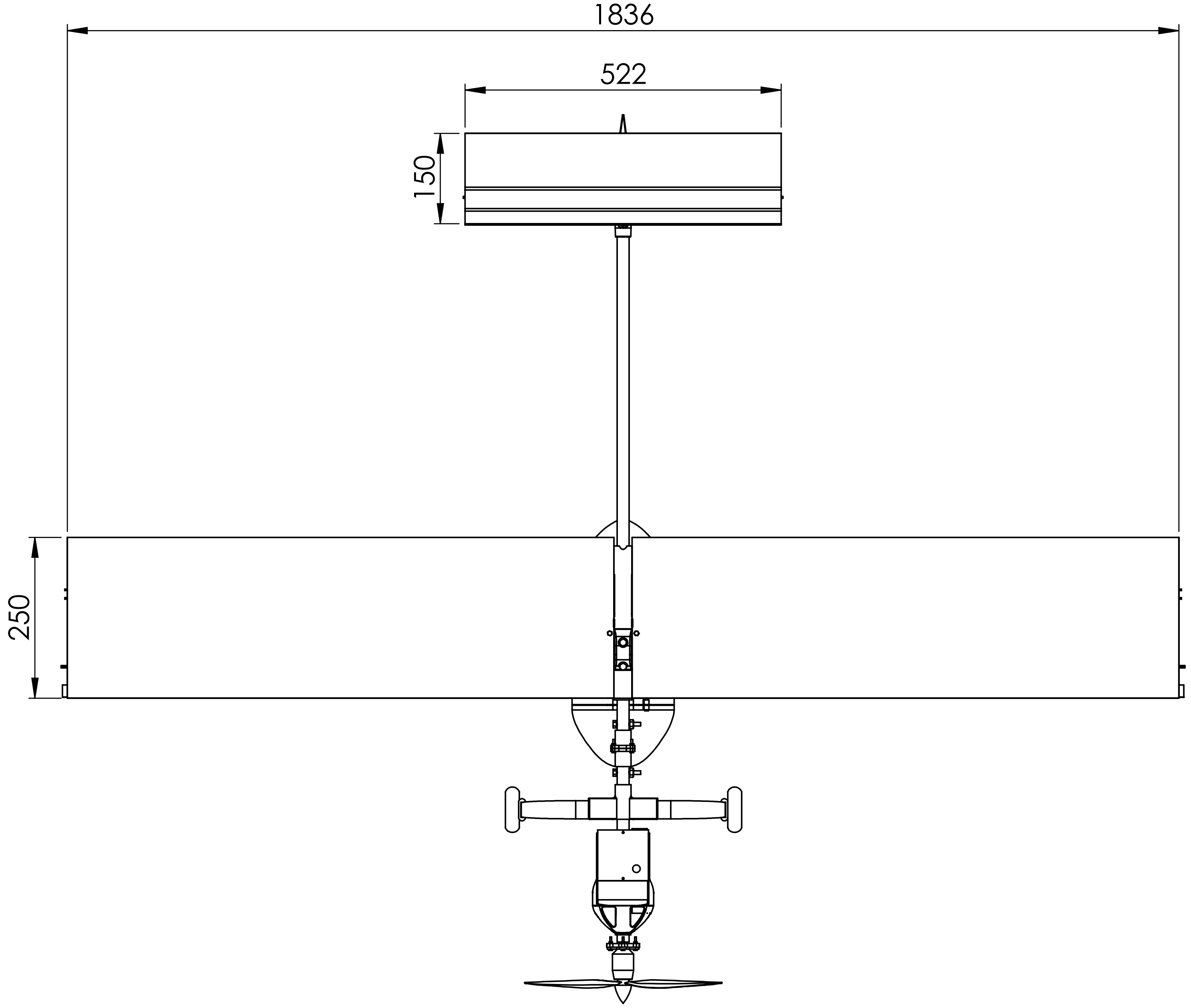

WING	
AIRFOIL	TB16537
WING AREA	4590 cm^2

USABLE BAY VOLUME	1584 cm^3

PAYLOAD DIMENSION	
LENGHT	190 mm
HEIGHT	110 mm
SINGLE BAG WIDTH	25 mm
SINGLE BAG WEIGHT	300 g
N° BOX	4

TITLE: LP1 VIEWS			
CODE: LP1_01			
DRAWN BY: LEANING PROJECT		MATERIAL:	WEIGHT: 3800g (EMPTY)
SCALE:1:12	REV: 02 SHEET 1 OF 1	GENERAL ROUGHNESS:	NOT INDICATED TOLERANCES: ±0,2 ±0,5°

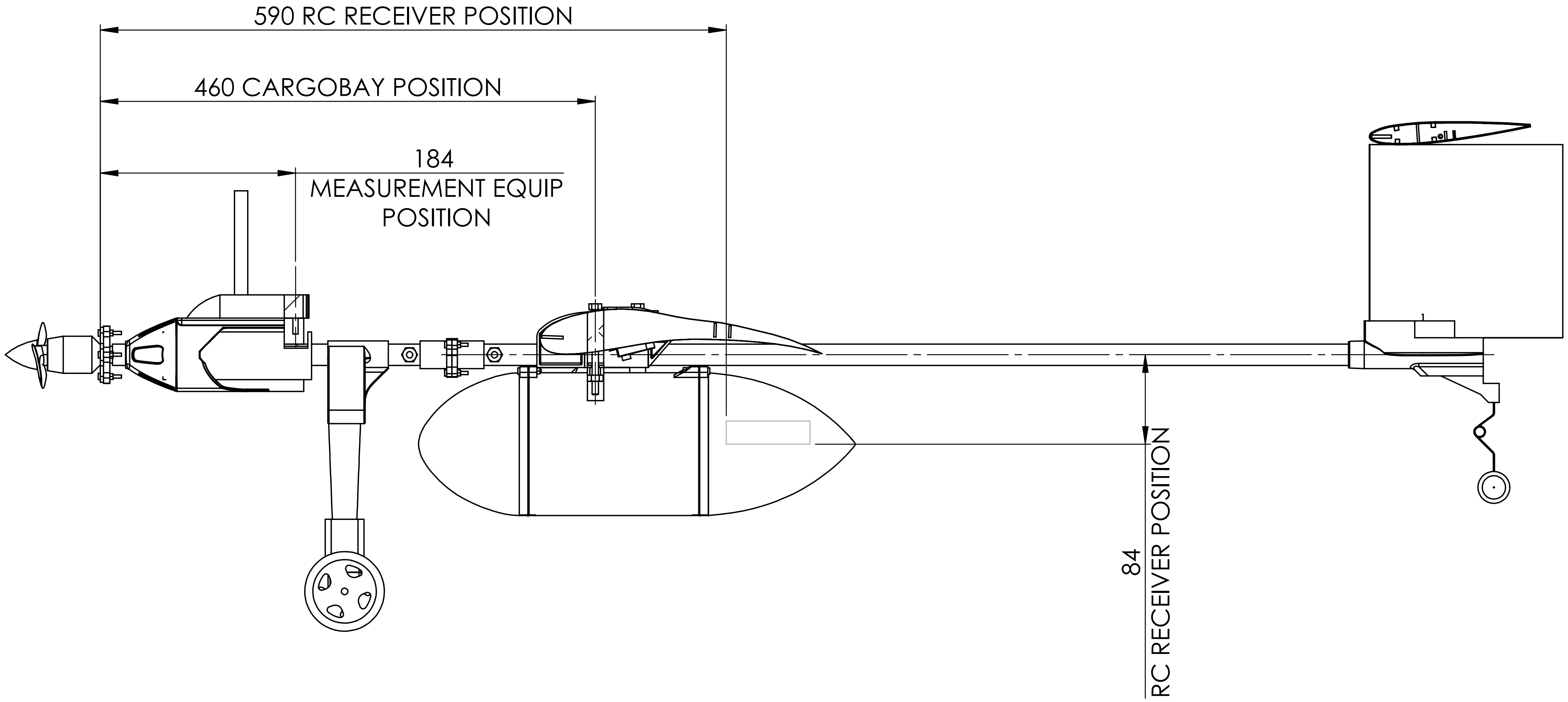

NOTE:

- ALL MEASURAMENT IN THIS SHEET ARE INTENTED ON MAIN FIXING FEATURES OF THE EQUIPEMENT CONSIDERED.
- ALL THE EQUIPMENT'S CoG ARE POSITIONED ON MID PLANE OF THE AIRCRAFT.

TITLE:	CARGOBAY & EQUIPEMENT POSITION
CODE:	LP1_01
DRAWN BY:	LEANING PROJECT
MATERIAL:	
WEIGHT:	
SCALE:1:5	
REV:	02
SHEET 1 OF 2	
GENERAL ROUGHNESS:	
NOT INDICATED TOLERANCES:	

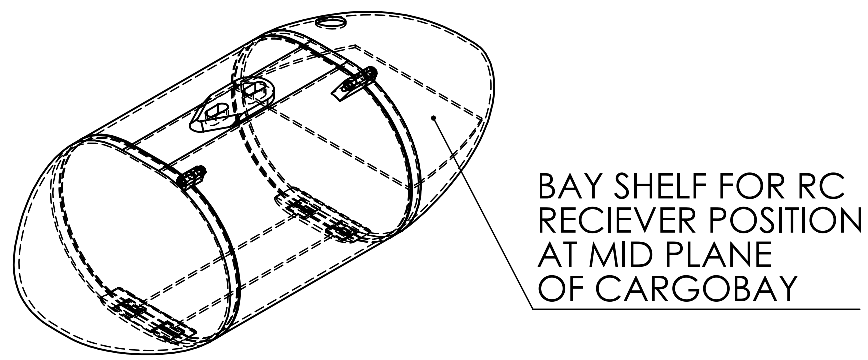

ISO VIEW FOR REFERENCE ONLY

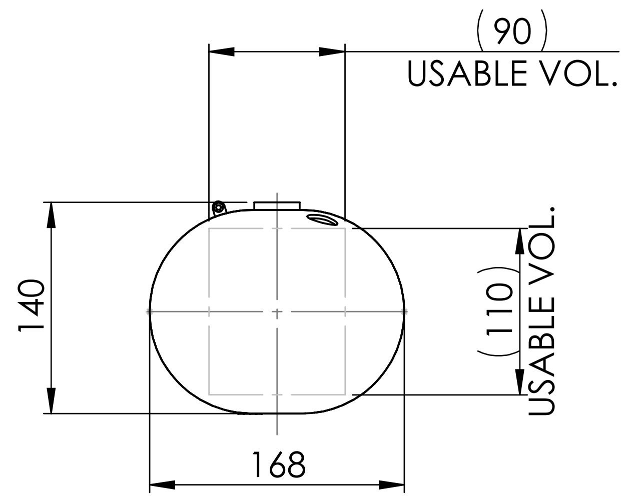

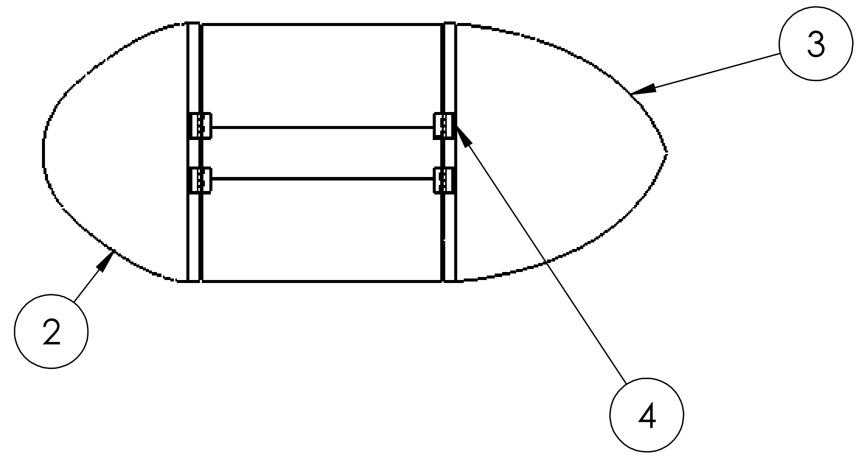

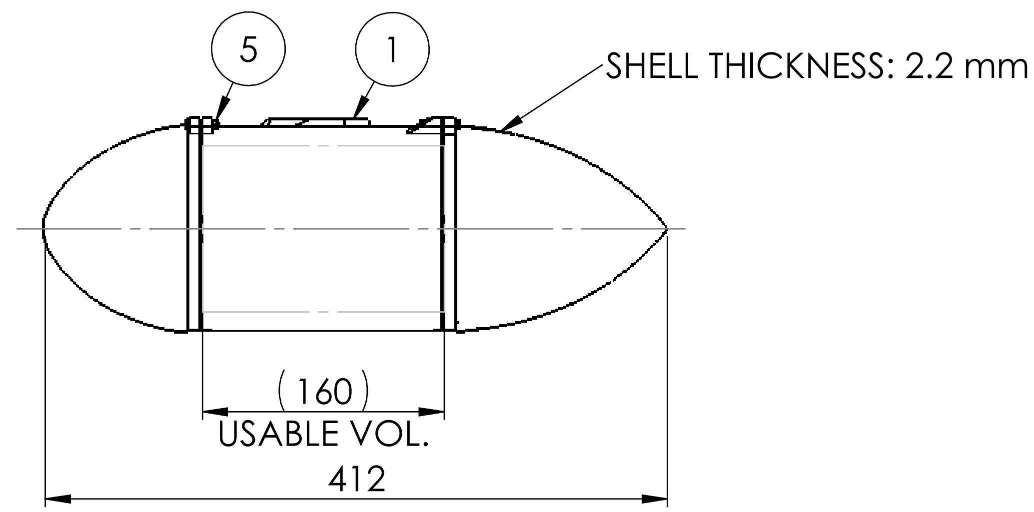

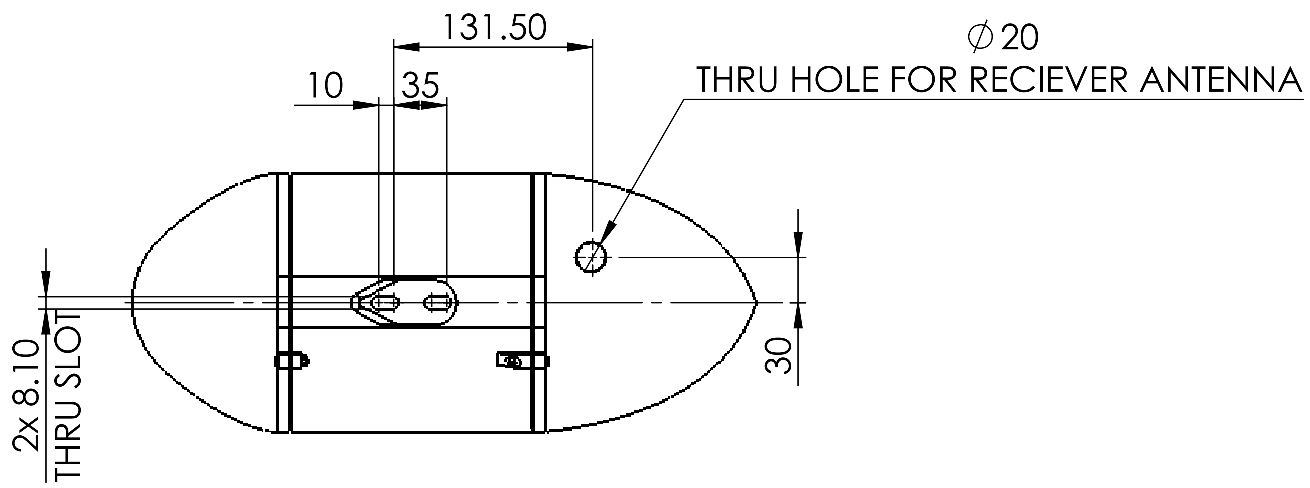

USABLE BAY VOLUME	1584 cm^3

PAYLOAD DIMENSION	
LENGHT	190 mm
HEIGHT	110 mm
SINGLE BOX WIDTH	25 mm
SINGLE BOX WEIGHT	300 g
N° BOX MAX	4

5	FIXING BOLTS	2
4	HINGE	4
3	REAR COVER	1
2	FRONT COVER	1
1	MAIN BODY	1

TITLE: CARGOBAY & EQUIPEMENT POSITION			
CODE: LP1_01			
DRAWN BY: LEANING PROJECT		MATERIAL: SEE BOM	WEIGHT: 470g
SCALE 1:5	REV: 02 SHEET 2 OF 2	GENERAL ROUGHNESS:	NOT INDICATED TOLERANCES: 0,2 0,5°

LEANING PROJECT

ITEM NO.	DESCRIPTION
1	FUSELAGE
2	WINGS
3	HORIZONTAL STABILIZER
4	VERTICAL TAIL
5	PROPELLER UNIT
6	CARGO BAY
7	TEFLON ATTACHMENT

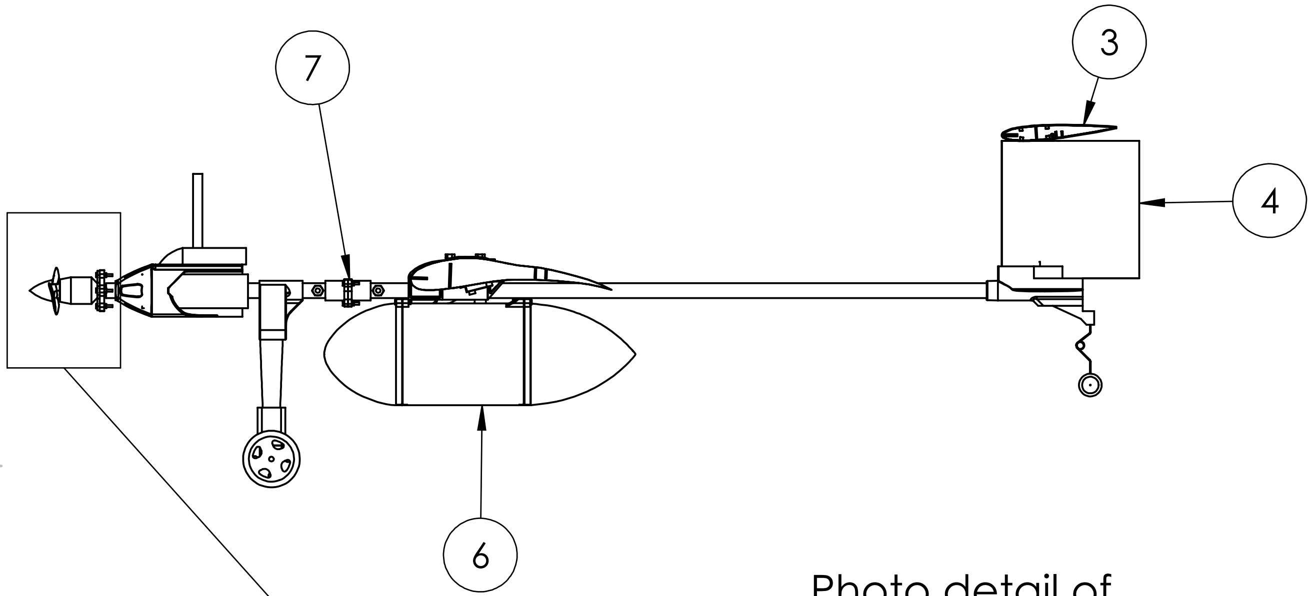

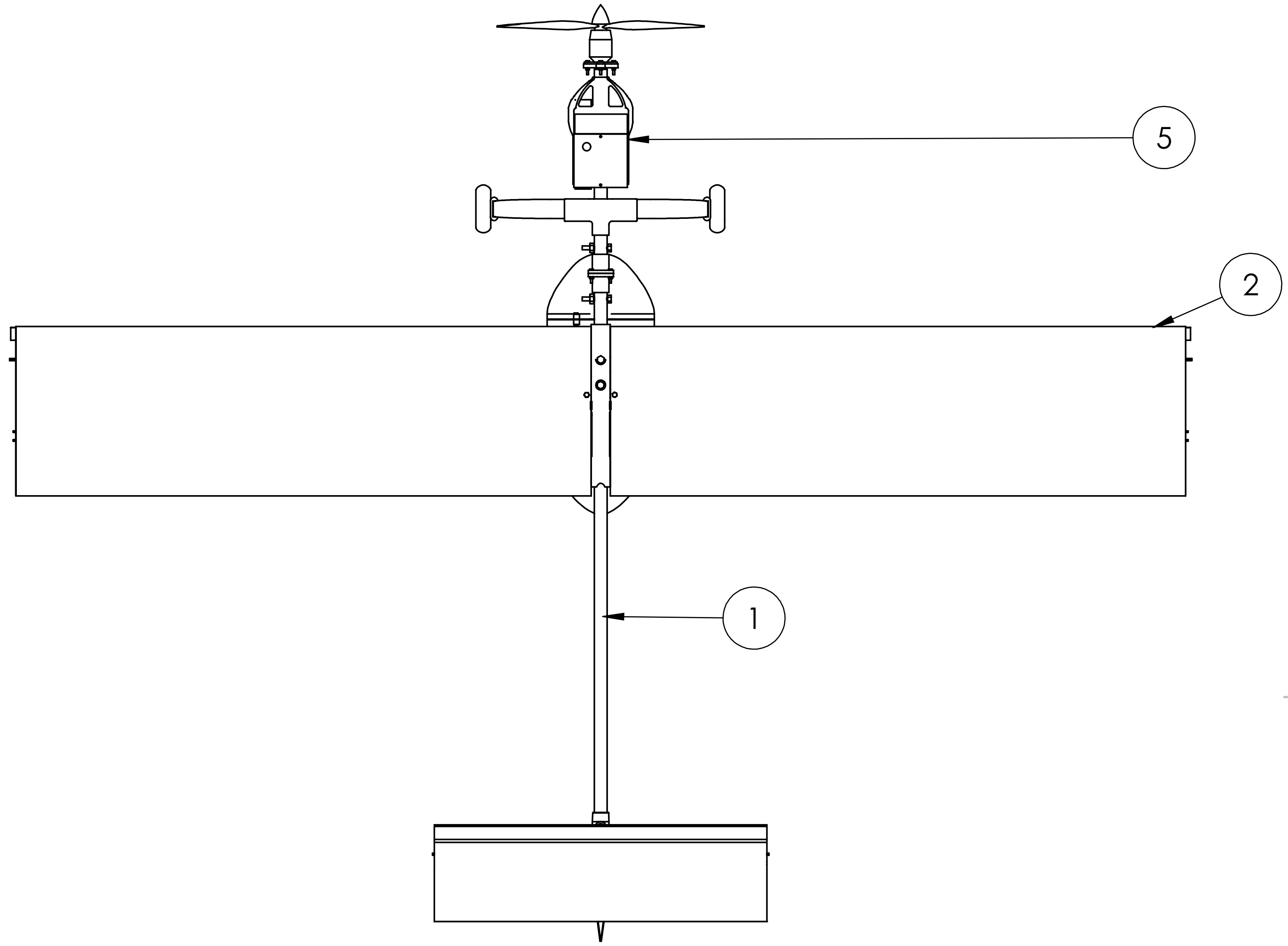

Photo detail of the propeller fastened to the power train.

TITLE:	LP1 MAIN ASSEMBLY
CODE:	LP1_01
DRAWN BY:	LEANING PROJECT
SCALE:1:10	REV: 02
	SHEET 1 OF 3

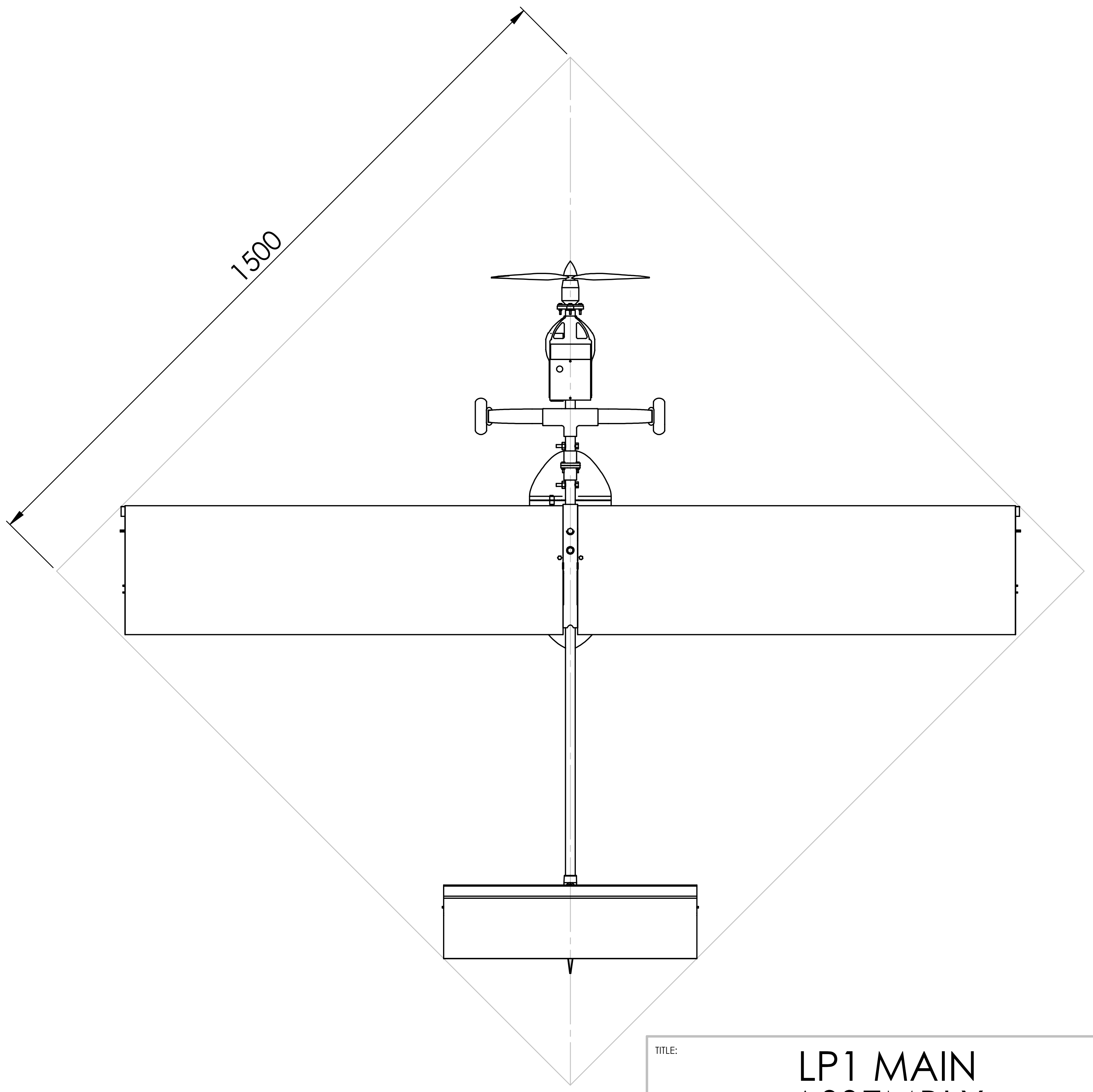

TITLE:	LP1 MAIN ASSEMBLY
CODE:	LP1_01
DRAWN BY:	LEANING PROJECT
SCALE:1:10	REV: 02
	SHEET 2 OF 3

LEANING PROJECT

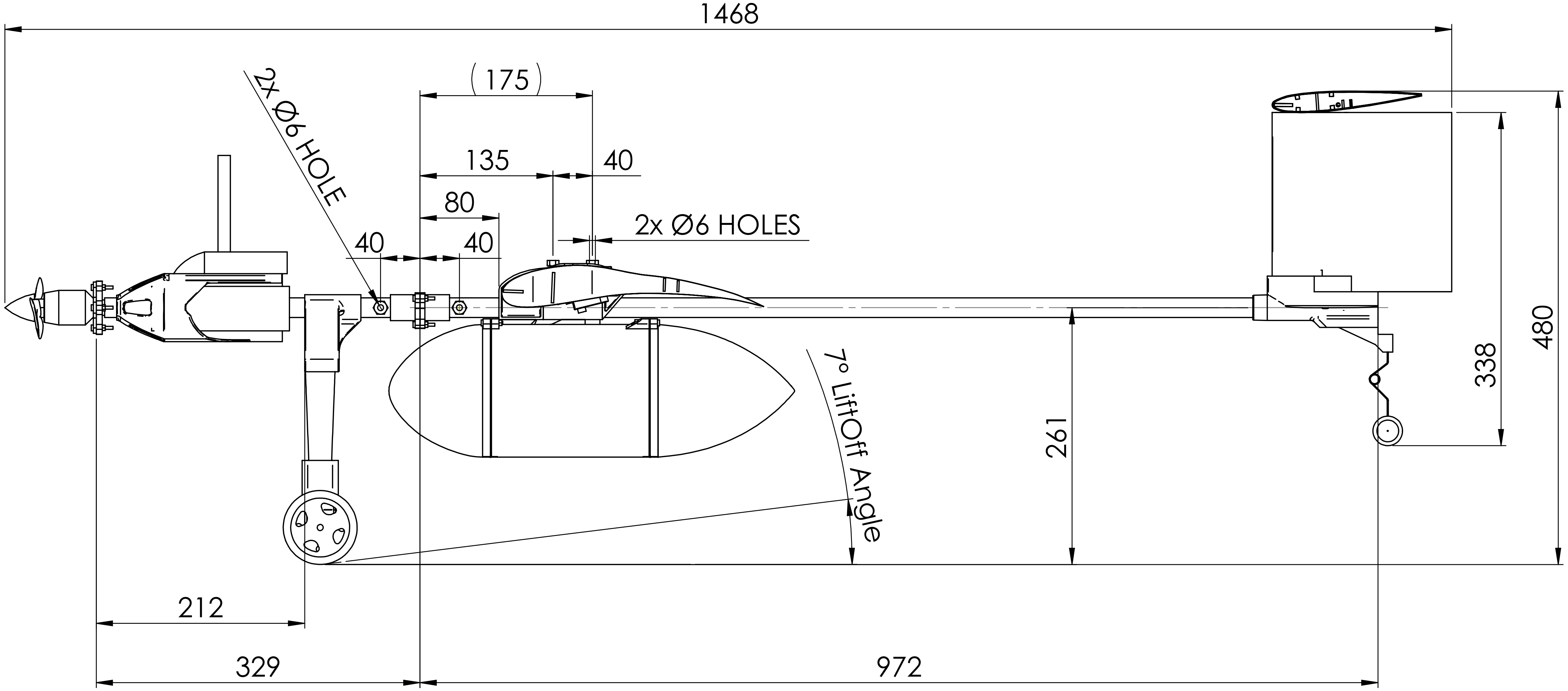

TITLE:	LP1 MAIN ASSEMBLY
CODE:	LP1_01
DRAWN BY:	LEANING PROJECT
SCALE:1:5	REV: 02
	SHEET 3 OF 3